NTNU
Det skapende universitet

Optimal kontrol av kontrollerbar pitch propell

Anders Brevik

Master i kybernetikk og robotikk
Innlevert: januar 2016
Hovedveileder: Tor Arne Johansen, ITK

Norges teknisk-naturvitenskapelige universitet
Institutt for teknisk kybernetikk

Problem Description

Optimal control of controllable pitch propeller
The best combinations of rpm and pitch are found using open-water tests and simulations: The propeller curve describes the combination between propeller rpm and shaft power for different pitch values. The combinator curve is determined from the best combinations at different powers and used in the thrust control scheme. However, during operation there are several effects that may change the optimal working point for the propeller. The goal of this project is to design a controller that optimally controls the pitch such that the best combination of rpm and pitch is used to produce the desired propeller force. The design may encompass estimator design and adaptive controller terms.

1. Design a controller that optimally controls the pitch such that the best combination of rpm and pitch is used to produce the desired propeller force.

2. Design an advance speed estimator.

Abstract

In recent years exciting advances have been made with controllable pitch propellers. This thesis' main goal is to design a controller that finds the optimal combination of shaft speed n and pitch diameter ratio P/D for different desired thrust values. The designed controller attempts to do this by utilizing inbuilt MATLAB solvers and optimized the open water efficiency of the propeller given values of the advance speed V_a and desired thrust T_d.

The second goal is to design an observer for the advance speed, this is done by using a MATLAB solver to find the value of the advance speed given measurements of propeller torque and the propeller inputs.

The results indicates that the controller is capable of eventually matching the desired thrust levels whilst using the estimate for advance speed, but it does so however at a non-optimal level of open water efficiency. It is concluded that rather than finding an optimal point given desired thrust and advance speed, an optimal path up to and including the optimal point should be made. The advance speed estimator is concluded to give good enough estimates for the controller in this thesis, it should however be fine-tuned for use in other, improved controllers.

Sammendrag

I senere år har det blitt gjort store framskritt innenfor propeller med kontrollerbar pitch. Hovedmålet til denne masteroppgaven er å designe en kontroller som finner den optimale kombinasjonen av akslingshastighet og "propellpitch" for en gitt verdi av ønsket thrust. Den designede kontrolleren forsøkte seg på dette ved å bruke innebygde "MATLAB-solvers" til å optimere ligningen for "open water efficiency", mens den holder seg innenfor verdiene som må til for å skape ønsket thrust gitt en "advance speed".
oppgavens andre mål er å lage en estimator som ved hjelp av dreiemomentsmålinger på propellen og viten om propellens inngangsverdier kan regne ut hva verdien for "advance speed" må være. Estimatoren tar og i bruk innebydge funksjoner i MATLAB.
Resultatene indikerer at selv om propellen klarer å generere de ønskede verdiene av thrust, gjør den så suboptimalt. Konklusjonen er at kontrolleren trenger en bedre løsning på hvordan den skal nå det optimale den punktet, da det å generere en optimal vei til et optimalt punkt er mest sannsynlig en mye bedre måte å gjøre det på. Det konkluderes også med at estimatoren fungerer bra nok for kontrolleren i denne oppgaven, men burde finjusteres for videre bruk.

Table of Contents

List of Figures

List of Tables

Glossary

Boss a propeller boss is the central portion of the screw propeller. It carries the blade and is connected to the propeller shaft.

Windmilling is when a propeller is not powered, but is free to move with external forces.

Acronyms

CPP Controllable Pitch Propeller.

DOF Degree of Freedom.

FPP Fixed Pitch Propeller.

FPS Frame per Second.

OWE Open Water Efficiency.

RPS Revolutions per Second.

Nomenclature

$\bar{n}$	Measured propeller shaft speed
$P\bar{/}D$	Measured pitch diameter ratio
$\bar{Q_p}$	Measured propeller torque
$\bar{V_a}$	Measured Value of Advance Speed
η	Tunable controller parameter
η_o	Open Water Efficiency
$\hat{V}_a$	Estimated Value Advance Speed
∇	Volume
ϕ	Boundary Layer Thickness
ρ	Water Density
σ	Surge reference error
A_e/A_o	Blade Area Ratio
B	Beam of the ship
C_b	Block Coefficient
D	Propeller Diameter
I_z	Moment of intertia about the z_b axis
J	Advance Ratio
K_i	Integral gain
K_p	Proportional gain

K_q	Propeller Torque Coefficient
K_t	Propeller Thrust Coefficient
L_{wl}	Length of the waterline
m	Mass of the ship
n	Propeller Shaft Speed
$N_{\dot{r}}$	Hydrodynamic derivative
p	Roll
P/D	Pitch Diameter Ratio
q	Pitch
Q_m	Motor Produced Torque
Q_p	Propeller Torque Load
$Q_{m,max}$	Max Limit of Motor Produced Torque
Q_{m_p}	Desired motor torque
r	Yaw
T	Draft of the ship
T_d	Desired Thrust
T_p	Thrust Produced
u	Surge
v	Sway
V_a	Real Value of Advance Speed
v_r	Relative velocity vector
w	Heave
w	Wake Fraction
x_g	Relative position of x to the center of gravity
$X_{\dot{u}}$	Hydrodynamic derivative
$Y_{\dot{r}}$	Hydrodynamic derivative
$Y_{\dot{v}}$	Hydrodynamic derivative
z	Number of Propeller Blades

Chapter 1

Introduction

Since the early days of man, he has had a special relationship with the sea and the ships he made to traverse them. Ships have been used to explore, work the ocean and transport both goods and people. These ships were in the earliest days, powered either by wind or manpower. During the eighteenth century, but even more prevalent in the nineteenth, ships became powered by steam engines. In the twentieth century, as the steam engines became diesel powered steam turbines, diesel costs started to rise, giving way for the reciprocating diesel engine found on most modern ships. But now, in the dawn of the twenty-first century, the diesel-electric propulsion system is starting to take its hold. The diesel-electric propulsion offers lower fuel consumption, higher efficiency and reduced life cycle cost.

Many of these modern electric-diesel marine vessels are fitted with Controllable Pitch Propellers (CPPs), these propellers are relied upon to provide thrust at a high efficiency in multiple operating conditions, providing better flexibility than the Fixed Pitch Propellers (FPPs). The main focus of this thesis will be to develop a consolidated control scheme, whose goal it is to provide the propeller with good inputs enabling its ship to accurately follow a surge reference at high Open Water Efficiency (OWE).

1.1 Background

Propellers with variable pitch have been around for a long time and have been used for numerous applications. Including air planes, turbines and pumps. But most important for this thesis are the ship applications. Propellers can be split into two major categories, Controllable Pitch Propellers (CPPs) and Fixed Pitch Propellers (FPPs). The Fixed Pitch Propeller is a solid cast propeller, optimized for a specific operating point. These types of propellers are usually installed on marine vessels which run at specifics speeds for long stretches of time. Such as container vessels, tanker ships and similar. But they do also see much use in smaller pleasure crafts and outboard motors. The Controllable Pitch Propeller first appeared on sailboats, where they were favoured for their ability to windmill with little resistance by pitching the propeller blades with the water flow. Back

then they had to be manually set whilst out of the water, but as time went on modern CPPs (example seen in figure 1.1) are now controlled remotely under operation. On the modern CPP the propeller blades can rotate by means of hydraulic mechanisms contained inside the propeller Boss. These mechanisms makes the propeller boss larger on CPPs than on FPPs. The bigger boss decreases efficiency and is a source of cavitation. Which are some of the reasons for why the FPP is still favoured for long ocean hauls. The CPPs most prominent ability, is to alter their optimal operating point. This makes the CPP especially suited for operations where the ship is subject to varying load conditions and environmental factors. They are also well suited for vessels that have frequent stops, such as ferries.

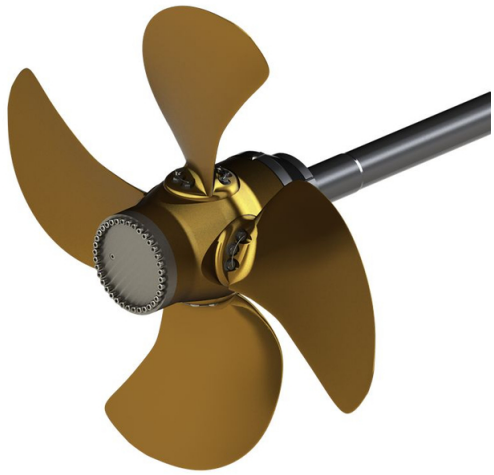

Figure 1.1: An illustration of a modern Controllable Pitch Propeller, courtesy of Schottel (2010).

1.2 Motivation

A common way to utilize the controllable pitch propeller has been to keep the shaft speed constant whilst relying solely on changes in pitch to produce the desired thrust. This controller scheme has proven itself to be very convenient when used in combination with electrical power generation, however having only one control variable may lead to inefficient performance and complicated cavitation characteristics. In this thesis however, an attempt is made to utilize the fact that the CPP can vary its optimal operating point. The different optimal operating points are visualized in figure (1.2) where the OWE curves of a CPP have been plotted. In figure 1.2, the advance ratio (2.4) runs along the x-axis and is a function of the propeller's diameter, the propeller's shaft speed and the propeller's advance speed. The larger the value of OWE is, the better the efficiency is at a certain advance ratio.

The curves are functions of three variables, the advance speed, which will have to be measured or estimated, the shaft speed n and the propeller pitch diameter ratio,P/D,

both of which can be controlled. So instead of merely having one control input, two are to produce the desired thrust and to also keep the propeller at its optimal operating point. If implemented properly, this type of control scheme, called consolidated control, promises better efficiency, faster acceleration and increased manoeuvrability.

1.3 Assumptions

In order to simplify the task at hand whilst still remaining true to the intent, the following assumptions and simplifications have been made:

- That the propeller characteristics of the Wageningen B-series can be used as the basis for an imaginary controllable pitch propeller. This has to be assumed as the results from similar tests done one CPPs are not readily available.
- Absence of both ventilation and cavitation. Ventilation is when the propeller pulls air from the surface and into itself. This lessens the torque load on the propeller, causes disturbances in performance and makes the control problem much harder. Cavitation is air bubbles caused by large pressure differences complicating the control problem further.
- Calm seas and zero in and out of water effects, i.e. the propeller stays fully submerged.

1.4 Contribution

The main contributions of this thesis are:

- A ship model with propeller modelling has been programming in a class based MATLAB script.
- A controller finding an optimal combination of propeller shaft speed n and pitch diameter ratio P/D for a given thrust reference and advance speed has been designed. This controller has been implemented with the ship in MATLAB.
- An estimator of advance speed has been design, it has been implemented in MATLAB.

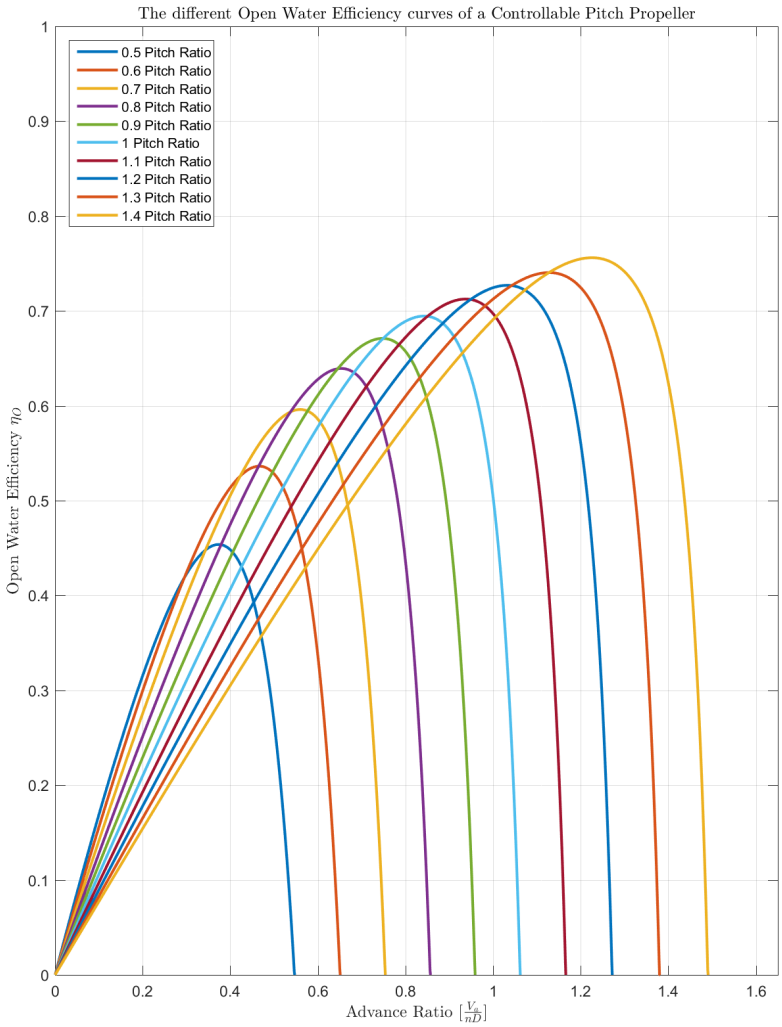

Figure 1.2: A plot showing the Open Water Efficiency curves of a Controllable Pitch Propeller.

1.5 Outline of thesis

The following chapters are outlined as such:
Modelling: In the modelling chapter key equations and variables relating to propeller modelling will be examined and explained. An explanation of the motor modelling will also be given, followed by a presentation of the ship model used in this thesis and some key coefficients regarding the hull shape of the ship.
Control and observer design: In chapter 3 this thesis' controllers and observer will be presented. Three controllers have been designed, one surge speed controller, one shaft speed controller and one controller which is responsible for propeller inputs, referred to as the consolidated controller.
Simulation and Results: In the results chapter, the results from four different test scenarios will be presented. The test scenarios are designed to see how the system responds to two different surge speed references, with measured advance speed $\bar{V}_a$ and with estimated advance speed $\hat{V}_a$ so that one can observe how the system responds to operating with an estimate.
Discussion: In this chapter, the results from chapter 4 will be further scrutinized and an emphasis will be placed on discussing the change in system performance caused by utilizing an estimate for the advance speed.
Conclusion and Further Work: In the final chapter there will be a brief conclusion of the work done and suggestions for improvements and ideas for further work will be presented.

Chapter 2

Modelling

2.1 Propeller

When modelling propellers for use in ship simulation, two central equations are the ones regarding the produced thrust and the propeller torque load.

$$T_p = \rho D^4 n|n|K_t \tag{2.1a}$$

$$Q_p = \rho D^5 n|n|K_q \tag{2.1b}$$

Both of these equations are found in Fossen (1994). From the equations (2.1a) and (2.1b) we have T_p, which is thrust produced by the propeller, Q_p which is the propeller torque load, ρ is the density of water, D is the diameter of the propeller and n is the shaft speed of the propeller i.e. the propeller Revolutions per Second (RPS). Finally there are the two coefficients, K_t and K_q which are the thrust and torque coefficients respectively. These coefficients were originally found from testing done on the Wageningen B-series propellers (M.M Bernitsas, 1981). The Wageningen B-series propellers are not CPPs, but rather FPPs, nevertheless they will be used for the CPP in this thesis as test results for CPPs are not available for the public.

2.1.1 Finding the K_t and K_q coefficients

Extensive testing with the Wageningen propeller (M.M Bernitsas, 1981) series was done at the Netherlands Ship Model Basin in Wageningen. A paper written by M.M Bernitsas (1981) is heavily relied upon in this thesis for finding values for thrust and torque coefficients used in propeller controller. The values for the K_t and K_q coefficients are given by the sums (2.2).

$$K_t = \sum_{s,t,u,v} C^T_{s,t,u,v}(J)^s(P/D)^t(A_E/A_o)^u(z^v) \tag{2.2a}$$

$$K_q = \sum_{s,t,u,v} C^Q_{s,t,u,v}(J)^s(P/D)^t(A_E/A_o)^u(z^v) \tag{2.2b}$$

In the sums (2.2), the two variables $C^T_{s,t,u,v}$, $C^Q_{s,t,u,v}$ and the exponents s, t, u and v are all constants. These constants are given in the appendix by the table in figure A.2. Further we have A_E/A_O, z and P/D, which are propeller design variables, with the latter one being controllable for the CPP. These design variables are the blade area ratio, the number of propeller blades and the pitch diameter ratio respectively. In the sums (2.2) J is the advance ratio, further explained in section 2.1.3.

The blade area ratio is the total surface area of the propeller blades divided by the circle area of the propeller, given by its diameter.

The pitch diameter ratio is the ratio of the propeller pitch to the diameter of the propeller. Pitch is short for blade pitch, which refers to the propeller blade's angle of attack. Pitch can be explained with imagining a wood screw. The larger the pitch of the screw thread the further it would travel into the wall per revolution. As the experiments done in M.M Bernitsas (1981) were done one propellers with a fixed P/D between 0.5 and 1.4, this thesis will use the same limits for P/D.

2.1.2 Pitch Dynamics

The pitch dynamics for the propeller are for practical purposes modelled as a first order system in this thesis, as in equation (2.3).

$$\dot{P/D} = \frac{P/D_d - P/D}{\tau_{p/d}} \tag{2.3}$$

In equation (2.3) P/D_d is the desired pitch diameter ratio and $\tau_{p/d}$ is a time constant.

2.1.3 Advance ratio

Advance ratio is a term used both in aeronautics and in marine hydrodynamics. The advance ratio of a propeller is a measurement of how far the propeller travels forwards through a medium during one revolution divided by the diameter of the propeller. In other words, it can be described as the speed of which the propeller moves through a medium, relative to the RPS of the propeller times the diameter, as described by equation (2.4).

$$J = \frac{V_a}{nD} \tag{2.4}$$

Here we have V_a as the speed of advance, or advance speed. The advance speed is defined with the propeller as the frame of reference, which means that the advance speed is the speed of which water enters the propeller. D is the propeller diameter and n the propeller shaft speed.

2.1.4 Open Water Efficiency

The advance ratio J is also used in combination with the K_t and K_q coefficients to give the Open Water Efficiency of the propeller. This relationship is described in equation

Figure 2.1: Screen capture of a video demonstrating open water testing (Froudedude, 2009).

(2.5).

$$\eta_O = \frac{J}{2\pi}\frac{K_t}{K_q} \tag{2.5}$$

Open Water Efficiency is the efficiency at which the propeller is operating in open water conditions and is a commonly used metric in propeller testing. Open water conditions means that the testing is done in a homogeneous wake field where the propeller is unhindered by the hull i.e. no hull interaction. See figure 2.1 for an example of open water testing.

2.1.5 Advance speed

In this thesis, a rough estimate of the advance speed given by equation (2.6) will be used as the value for the real advance speed in the simulation. In section 3.4 we will look at how the advance speed can be estimated for control purposes.

$$V_a = (1 - w)u \tag{2.6}$$

In equation (2.6) u is the ship's velocity in surge and w is the wake fraction, a function of the hull shape. The wake fraction will be further explained in section 2.3.2.

2.1.6 Quadrant Dynamics

Propellers are said to be operating in one of four quadrants. The quadrants are defined in table 2.1

In this thesis, we will only operate the propeller in the first quadrant, i.e. the propeller will never spin in the negative direction and the propellers advance speed is always positive. The reason for choosing to operate only in the first quadrant is to simplify the system, as the thrust and torque coefficient calculations become much more complicated if one is to take a full four-quadrant model into consideration.

Table 2.1: The four quadrants of propeller operation, defined with the advance speed V_a and shaft speed n.

	1st	2nd	3rd	4th
V_a	≥ 0	< 0	< 0	≥ 0
n	≥ 0	≥ 0	< 0	< 0

2.2 Motor

In recent years, diesel-electric propulsion is becoming a increasingly popular choice when designing ships. As the world is going green, the diesel-electric promise of lowered fuel consumption and emissions is more popular than ever. By having the diesel engines running at optimal load conditions and at a constant rate, fuel efficiency is greatly optimized (MAN Marine Engines & Systems, 2012). Diesel-electric propulsion also comes with added bonuses such as lower propulsion noise and a reduction in vibrations. The diesel-electric propulsion system is even more reliable than a standard reciprocating diesel engine, partly due to the ease of which it can be designed with redundancy in mind.

It is because of these advantages, and the author's partiality to electric motors in general, the propulsion plant in this thesis is thought of to be a diesel-electric one. The diesel engines are not modelled, and they are assumed to provide the electric motor with as much power as is required. The electric motor is thought of as a electric AC-motor with variable speed drive. An electric AC motor with variable speed drive is capable of delivering the desired torque in short time frame. This short time frame enables the modelling of the motor-propeller dynamics to be simplified. By doing it this way, the only elements needed to model the motor-propeller dynamics are the inertia of the axle and propeller, the torque delivered from the motor and the torque load on the propeller. This model can be described by:

$$J\dot{n} = Q_m - Q_p \tag{2.7}$$

It is assumed that the AC-motor is quick enough so that Q_m can be imagined to be produced instantly. I.e. the motor's sole constraint is an upper and lower limit on the torque production. To ensure that the propeller stays within the defined first quadrant, the motor is never allowed to exert a negative torque on the propeller axle. Motor torque, Q_m, is therefore within the bounds given by equation (2.8).

$$0 \leq Q_m \leq Q_{m_{max}} \tag{2.8}$$

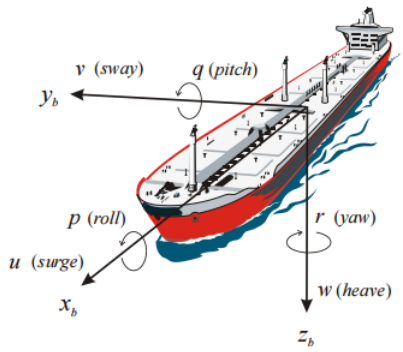

Figure 2.2: Illustration of the six degrees of freedom, image courtesy of Fossen (2015).

2.3 Ship

2.3.1 Three Degrees of Freedom ship model

From Fossen (2011) we have that the equations of motion with six Degrees of Freedom (DOFs) for marine crafts may be written on the form:

$$\dot{\eta} = \mathbf{J}_\Theta(\eta)\nu \tag{2.9a}$$

$$\mathbf{M}\dot{\nu} + \mathbf{C}(\nu)\nu + \mathbf{D}(\nu)\nu + \mathbf{g}(\eta) + \mathbf{g_0} = \tau + \tau_{wind} + \tau_{wave} \tag{2.9b}$$

where:

$$\eta = [x,\ y,\ z,\ \phi,\ \theta,\ \psi]^T \tag{2.10a}$$

$$\nu = [u,\ v,\ w,\ p,\ q,\ r]^T \tag{2.10b}$$

In equation (2.10a) η represent the position and heading of the ship, whilst in equation (2.10b) ν represents the ship's linear and angular velocity. The τ vectors represents forces and moments in the six DOFs. The matrix $\mathbf{M}$ contains the mass and inertia elements of the model, $\mathbf{C}(\nu)$ contains the Coriolis elements, and $\mathbf{D}(\nu)$ expresses the damping forces. Lastly, $\mathbf{g}(\eta)$ contains the generalized gravitational and buoyancy forces, the remaining static restoring forces and moments due to ballast system and water tanks are found in $\mathbf{g}_0$. In this thesis, the focus is on the propeller and its ability to generate accurate thrust values in order to for the ship to reach the value of the surge reference. For this purpose movements in heave and angular changes in roll and pitch are uninteresting. Because of this a model containing all the six DOFs is not needed and this thesis will instead rely on a simplified three DOFs model containing movements only in surge way and yaw. For this purpose a three DOF model based on rigid-body kinetics have been chosen. This means that the equations of motion will take the form of (2.11b).

$$\dot{\eta} = \mathbf{J}_\Theta(\eta)\nu \tag{2.11a}$$

$$\mathbf{M}\dot{\nu} + \underbrace{\mathbf{C}(\nu)\nu + \mathbf{D}(\nu)\nu}_{\mathbf{N}(\nu)\nu} = \tau + \tau_{wind} + \tau_{wave} \tag{2.11b}$$

where:

$$\mathbf{M} = \mathbf{M}_A + \mathbf{M}_{RB} \tag{2.12}$$

$\mathbf{M}_A$ is the mass and added mass matrix, added mass is a term used in fluid mechanics to take into account the mass of a fluid which will need to be moved in order to move an object. In this case the added mass is the extra inertia caused by the water surrounding the ship. $\mathbf{M}_{RB}$ is the rigid-body inertia matrix. All of the terms in $\mathbf{M}_A$ and $\mathbf{M}_{RB}$ are inertia terms and they can there grouped together in in one matrix $\mathbf{M}$. The ship model being used is in this thesis is a nonlinear maneuvering model based on Second-order modulus functions, and is given by Fossen (2011). This model was chosen as it is suitable for models in motion and a good fit for this thesis, as this thesis will not go into the area of station-keeping. $\mathbf{N}(\nu)\nu$ is given by (2.13):

$$\mathbf{N}(\nu)\nu = \mathbf{C_a}(\nu)\nu + \mathbf{D}(\nu)\nu \tag{2.13}$$

Fully expanding the equation of motion (2.11b):

$$\begin{bmatrix} m - X_{\dot{u}} & 0 & 0 \\ 0 & m - Y_{\dot{v}} & mx_g - Y_{\dot{r}} \\ 0 & mx_g - Y_{\dot{r}} & I_z - N_{\dot{r}} \end{bmatrix} \begin{bmatrix} \dot{u} \\ \dot{v} \\ \dot{r} \end{bmatrix} + \\ \begin{bmatrix} -X_{|u|u}|u_r| & 0 & Y_{\dot{r}}v_r + Y_{\dot{r}}r \\ 0 & -Y_{|v|v}|v_r| & -X_{\dot{u}}u_r - Y_{|v|r}|v_r| \\ -Y_{\dot{v}}v_r - Y_{\dot{r}}r & X_{\dot{u}}u_r - N_{|v|v}|v_r| & -N_{|v|r}|v_r| \end{bmatrix} \begin{bmatrix} u \\ v \\ r \end{bmatrix} = \tau \tag{2.14}$$

In equation (2.14) we have m which is the mass of the ship, $X_{\dot{u}}$, $Y_{\dot{v}}$, $Y_{\dot{r}}$ and $N_{\dot{r}}$ are all hydrodynamic derivatives, I_z represents the moment of inertia about the z_b axis and we have x_g which is the relative position in x to the center of gravity. Further, we have $X_{|u|u}$, $Y_{|v|v}$, $N_{|v|v}$, $Y_{|v|r}$ and $N_{|v|r}$ which represents nonlinear damping and lastly we have v_r which is the relative velocity vector to the current.

2.3.2 Wake coefficient and advance speed

The wake fraction is a factor indicating the speed of which the incoming velocity of the ship is seen by the propeller, as it is operating in the wake of the ship. In order to estimate the wake fraction, it is important to know by which means of propulsion the ship is moved. For this thesis, simulations are done on a single screw operated ship. This means that the ship will be moved by only one propeller, in comparison a twin screw operated ship uses two propellers. For a single screw operated ship, an estimate for the wake fraction can be found using an equation (2.15) from Taylor (1943).

$$w = 0.5C_b - 0.05 \tag{2.15}$$

In equation (2.15) C_b is the block coefficient of the ship. The block coefficient is one of the coefficients used to compare ship hull forms. The block coefficient is the ratio of the submerged volume of the ship compared to an imagined block made from ship

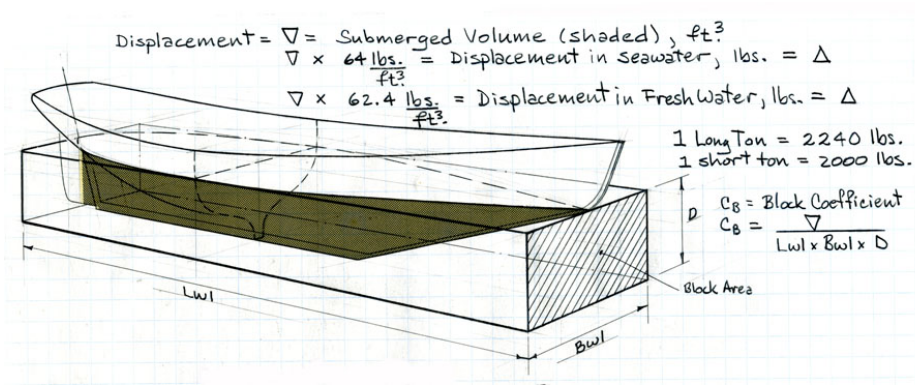

Figure 2.3: Illustration of a Block Coefficient calculation, figure courtesy Sponberg (2001).

measurements, see figure 2.3.
It should be noted that when using (2.15), high values of C_b will result in low values of wake fraction w compared to other equations used for estimating the wake fraction w using the same value for C_b. The block coefficient C_b is given by an equation found in K. J. Rawson (1976).

$$C_b = \frac{\nabla}{L_{wl}BT} \tag{2.16}$$

In the block coefficient equation (2.16) L_{wl} is the length of the waterline, which is the the distance along the waterline from the forward most point on the ship's profile to the stern-most point. B is the beam of the ship, the width of the hull and T is the draft, the distance from the waterline to the keel. These measurements are all also visible in figure 2.3.

Chapter 3

Control and observer design

In this thesis control is divided into three main parts.

- Speed Controller
- Consolidated Controller
- Propeller Shaft Controller

The speed controller attempts to match the ships surge with a reference surge, it outputs the desired thrust levels needed to reach and maintain the desired speed. This desired thrust is then fed into the consolidated controller, which in combination with an estimate for the advance speed outputs the optimal combination of pitch diameter ratio and shaft revolutions needed to create the desired thrust level. The propeller shaft controller governs the electric motor in charge of applying a torque on the propeller shaft and outputs a desired torque creating the desired shaft speed n_d. In addition, an assumption has been made that the propeller's pitch dynamics are so fast, that they do not need a controller and can be modelled as a first order system.

3.1 Speed control

For speed control, a forward speed controller (Fossen, 1994) of the form (3.1) has been chosen.

$$\tau = (m - X_{\dot{u}})\,\dot{u}_d + \frac{1}{2}\rho C_d A|u|u - (m - X_{\dot{u}})\,\eta \tanh\left(\frac{\sigma}{\phi}\right) \tag{3.1}$$

Here τ represents the desired thrust, C_d the drag coefficient, A as the projected area, σ is $u - u_d$, ϕ is the boundary layer thickness and finally we have η as a tunable parameter. The drag coefficient C_d in this case, is approximated as the 2-D drag coefficient. This works as testing in this thesis is limited to surge. The 2-D drag coefficient, C_d^{2D} is calculated in MATLAB with the MSS toolbox (mss, 2010) using the breadth and length values of the ship and the built in function *Hoerner*.

```
Cd = Hoerner(B,T)
```

This function uses Hoerner's curve in its computations. It is very important the the speed controller is tuned properly, as one has from Fossen (1994) that the desired accuracy of a speed controller needs to be roughly $0.05m/s$. A properly tuned speed controller also helps to avoid oscillations, which is important as oscillations increases power usage and drastically reduces the energy efficiency of the vessel.

To ensure that the propeller never leaves the first quadrant (see section2.1.6) a no-brake strategy will be adopted. A no-brake strategy is a means of decreasing the surge velocity by relying solely on external resistance. This means that the speed controller will have lower limit of zero placed on its desired thrust output.

3.2 RPS and shaft dynamics

As mentioned in section 2.2 the electric motor is assumed to have very rapid dynamics. This means that they can be ignored and that the exact torque required by the shaft speed controller is instantaneously (3.3) provided by the motor. The shaft speed controller takes the form of a common PI-controller (3.2).

$$Q_{m_d} = K_p e(t) + K_i \int_0^t e(t)dt \tag{3.2}$$

$$Q_m = Q_{m_d} \tag{3.3}$$

In (3.3) Q_{m_d} is the desired motor torque and Q_m is the delivered torque. In (3.2) K_p and K_i are tunable controller gains and e is the error signal, $n_d - n$.

3.3 Consolidated control

The consolidated controller is formulated as an optimization problem (3.4). The goal of this controller, is to maximize the Open Water Efficiency (OWE), η_O. The OWE is a function of three variables, the advance speed V_a, the shaft speed n and the pitch diameter ratio P/D. The same holds true for the desired thrust T_d. As the P/D and n are control variables, this is a solvable optimization problem.

$$\begin{aligned} \max_{\eta_O} \quad & \eta_O = \frac{J}{2\pi}\frac{K_t}{K_q} \\ \text{s.t.} \quad & T_d = \rho D^4 n|n|K_t \end{aligned} \tag{3.4}$$

When solved, this ensures that the combination of shaft speed n and pitch diameter ratio P/D will deliver the desired thrust, and at the same time maximize the potential OWE, η_O, of the propeller

3.4 Advance speed estimation

As it is very expensive and complicated to measure the advance speed, proper advance speed estimation is important for optimal ship performance. This can be done by using a technique found in Luca Pivano (2009). Here the advance speed is estimated by using measurements of the torque Q_p, the pitch diameter ratio P/D, of the propeller and the propeller shaft speed n (Luca Pivano, 2009). This is done by using the torque equation from (2.1b) and solving for V_a. Remember that K_q (2.2) is a function of, amongst other constants and variables, the advance ratio J and the propeller pitch diameter ratio, P/D. Since we know from section 2.1.3 that the advance ratio is expressed as:

$$J = \frac{V_a}{nD}$$

We can imagine the torque equation as (3.5):

$$Q_p = \rho D^5 n|n|K_q(n, P/D, V_a) \tag{3.5}$$

Since D and ρ are constant and we assume that Q_p, n and P/D are all available for measurement we can write (3.5) as:

$$\bar{Q}_p = \rho D^5 \bar{n}|\bar{n}|K_q(\bar{n}, \bar{P/D}, \hat{V}_a) \tag{3.6}$$

In (3.6), measurements are noted with $\bar{}$ and estimates with $\hat{}$.

With all other variables in (3.6) known, one can solve for an estimate of the advance speed V_a. To accomplish one might use the MATLAB solver *fmincon*.
However, in order for this calculation to work there had to be placed a limit on how slow the ship was moving in surge, compared to the shaft speed n. For the calculations to start, the shaft speed had to be larger than the surge velocity of the ship times a confidence factor of 0.2685 (3.7). The confidence factor's value was found by testing the validity of the estimate at different confidence factor values.

$$n > u \cdot 0.2685 \tag{3.7}$$

The reason for this conditions is that if the propeller is rotating slowly and the surge of the ship sufficiently large, the advance speed estimate becomes highly unpredictable and seldom usable.

Chapter 4

Simulation and Results

The physical models from chapter 2 and the controllers and estimator from chapter 3 were programmed in MATLAB using object oriented programming. The different models and controllers were split into the following classes:

1. Ship
2. Advance speed estimator
3. Speed controller
4. P/D and shaft speed controller (Consolidated Controller)
5. Propeller
6. Motor and shaft controller

Each of these classes had their own functions and variables, for example: The propeller class had functions calculating the produced torque, thrust etc based on its own class variables and input from other classes. Writing the model this way created an easily maintainable code with good readability and modularity. The ODE solver used to simulate the system was chosen to be *ODE23*, as this solver proved relatively fast and provided good results. Stiff solvers were tested, but provided unfavourable results.

4.1 Simulation Setup

The initiation for all test cases was the same, all state values except for surge speed u and pitch diameter ratio P/D were initiated as zero. Surge speed u was initiated as almost zero, at $0.01m/s$ and P/D was initiated to 1 as the P/D ratio had to be within 0.5 to 1.4, see section 2.1.1.
When run, the simulation first took the thrust produced by the propeller class and applied it to the ship class' equations of motion. Then the speed controller took the surge value

of the ship class and used it to calculate the desired thrust. After this, if applicable the advance speed was estimated for use in combination with the desired thrust to generate references for the P/D ratio and the shaft speed n, if not the measured advance speed was used. The P/D was then applied to the propeller before the propeller calculated the thrust and torque produced by the current values of P/D, n and V_a. Finally, the motor applied a torque given by the shaft speed controller before the state values of $\dot{\nu}$, $\dot{n}$, $(n_d - n)$ and $\dot{P/D}$ were integrated for use in the next iteration.
A time step of 0.1 seconds proved to be the optimal combination of accuracy and time consumption. But the simulation as a whole was not very time efficient. The largest factor in this might have been the fluctuations in thrust produced when the surge reference was reached. This is based on that the simulations usually slowed down considerably once the reference was met. The simulations done with the CPP and V_a estimator took the longest time to complete.

4.1.1 Test Cases

Since the main focus of this thesis is how the open water effectiveness of a propeller could be optimized by proper control. As thrust generating is the important aspect of this, test scenarios only involving surge are sufficient to prove intended results. In order to see what effect the control scheme had on the open water efficiency of the propeller the propeller controller was ran in two different modes. One with the pitch locked at 0.8, fixed pitch mode, and the other where it could set the pitch freely between 0.5 and 1.4, variable pitch diameter ratio. Since the values given in M.M Bernitsas (1981) were found by testing on propellers with pitch diameter ratios ranging from 0.5 to 1.4 the pitch diameter ratio will be constrained by these values in this thesis. It will also be assumed that the values given by M.M Bernitsas (1981) also holds true for all values of P/D between 0.5 and 1.4. The propeller set to be 3 meters in diameter, have 4 blades, a blade area ratio of 0.7 and its inertia is set to $10000\ kg \cdot m^2$. Both the controllable pitch propeller and fixed pitch propeller were tested in four different conditions. These conditions are presented in table 4.1.

Table 4.1: Overview of test scenarios

	$\bar{V}_a$	$\hat{V}_a$	Step ref	Sine ref
Test scenario 1	×		×	
Test scenario 2	×			×
Test scenario 3		×	×	
Test scenario 4		×		×

As can be seen in table 4.1, both controller modes were tested with both real values of V_a and estimated values of "Step" is a step given the MATLAB function:

```
heaviside(t-5)*5
```

and ”Sine” is a sine curve given by:

```
2+0.5*sin(0.05*t)
```

4.2 Simulation Results

4.2.1 Test Scenario 1

In figure 4.1 one can see how the two different controller modes manages to reach the reference surge, with the reference surge being a step function. One can also observe their respective OWE (higher is better). In this scenario the controller in charge of pitch and propeller shaft speed reference had access to the real advance speed of the ship. In figure 4.1 one can clearly see that both controller modes were successful in achieving the reference surge and holding it, albeit with a tiny overshoot. This overshoot however is within reasonable accuracy, see section 3.1. The fixed pitch mode reaches the reference faster than the controllable pitch mode, this is mirrored in the plot of the open water efficiency of their respective propellers. As one can see the fixed pitch mode settling on a higher value as it reaches the reference, the same as can be seen for the controllable pitch mode, when it reaches the reference. The extremely high values around $t = 0$ in the open water efficiency is merely a numerical oddity created by the ode solver and does not represent real values and should therefore be disregarded.

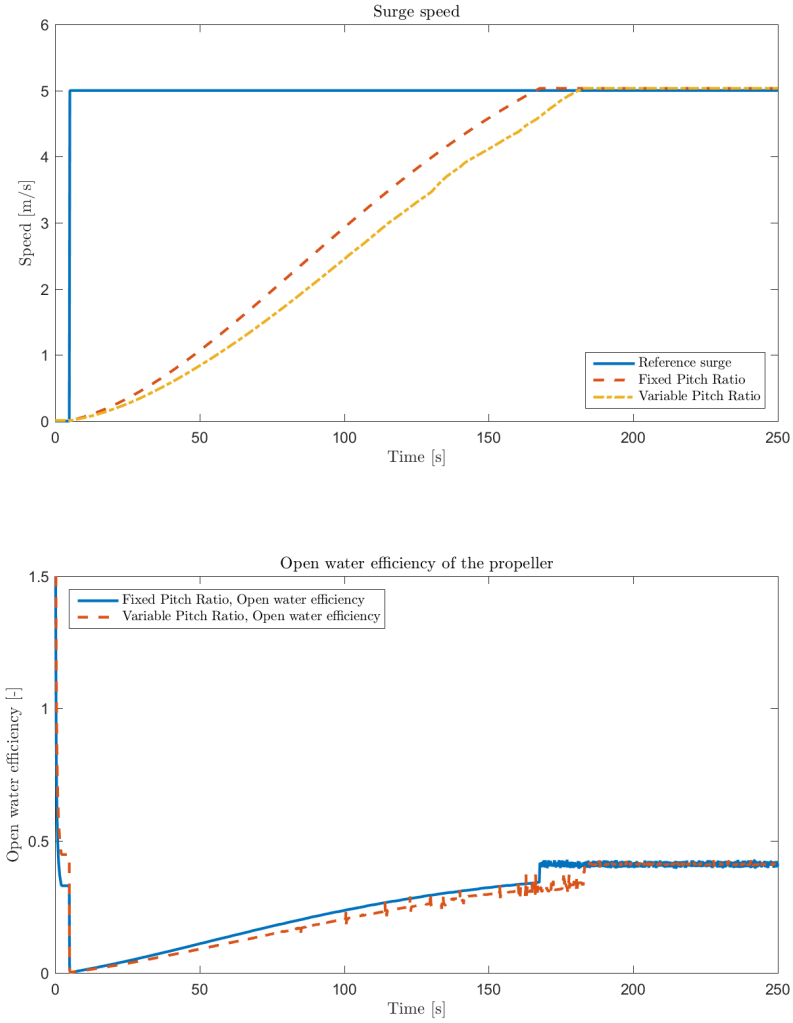

Figure 4.1: Results of test scenario one.

4.2.2 Test Scenario 2

In test scenario two the controller modes were subjected to a reference surge modelled as a sine wave. It can be seen in figure 4.2, the fixed pitch controller is the first to reach the reference value. When the reference is reached, both of the two modes matches the reference very well. However, as the reference value start decreasing after its second peak, it becomes clear that the controllable pitch controller manages to decrease its thrust faster than the fixed pitch controller, as both modes operate with a no-brake strategy, relying solely on resistance to slow down. This means that the ship equipped with the controllable pitch controller respond faster to the lessened surge reference.

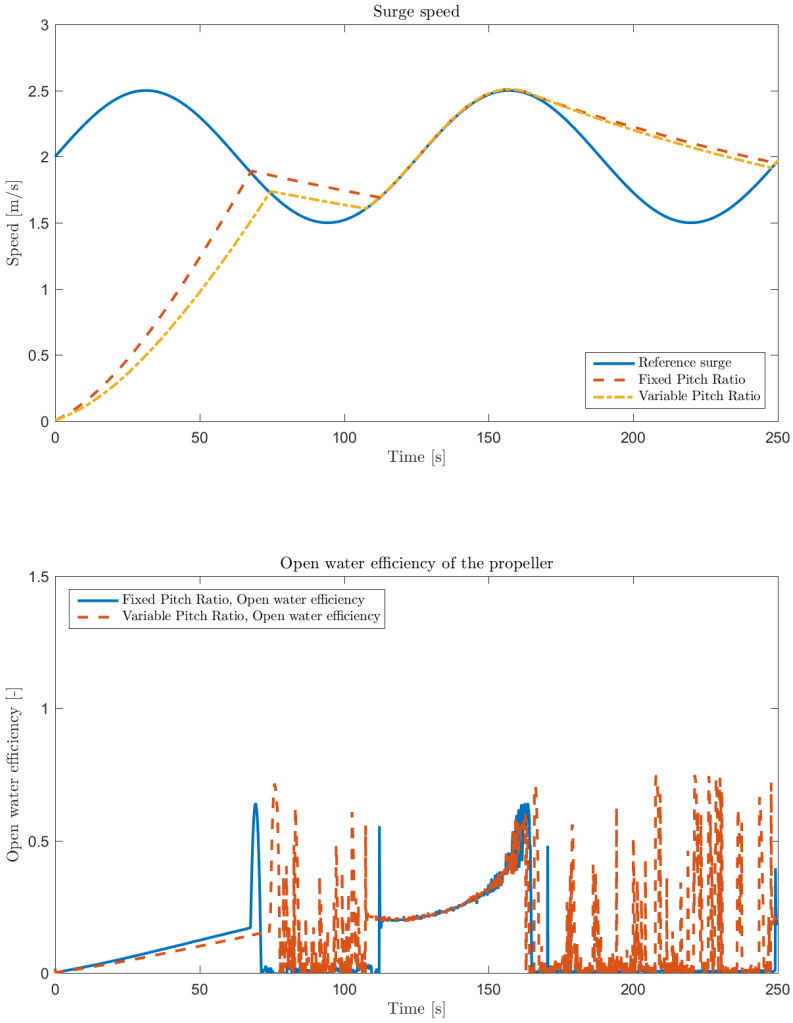

Figure 4.2: Results of test scenario two.

4.2.3 Test Scenario 3

For the third test scenario, a step response was used as in scenario one. However, in this scenario the controllers only had access to an estimate of the propeller's advance speed. Except for this, the conditions were identical in all other manners. When comparing the fixed mode controllers with real and estimated advance speed, one can see that they behave nearly identically. The fixed pitch mode in scenario one is able to reach the reference about 0.02 seconds earlier than the FPP in scenario three. The controllable pitch mode controller also behaves fairly similarly with the CPP in test scenario one. However with the estimated advance speed the controllable pitch controller struggles slightly more, creating a less stable values of surge. Nonetheless, by account of the less stable values the CPP reaches the reference surge approximately three seconds earlier than the CPP using measurements of the advance speed. It is worth noting the same trends regarding both the FPP's and the CPP's open water efficiency in test scenario one can also be observed in test scenario three.

Looking at the advance speed plots, one can see that the fixed pitch mode is better at estimating the advance speed of the propeller when rising than the controllable pitch mode has, but once the reference speed has been achieved this becomes untrue. For the FPP one can see large fluctuations and a rapidly varying estimate. The opposite can be seen for the controllable pitch mode controller, here the estimate becomes better once the reference speed has been met. There are however, also some fluctuations here as well, although they are more common during the surge acceleration.

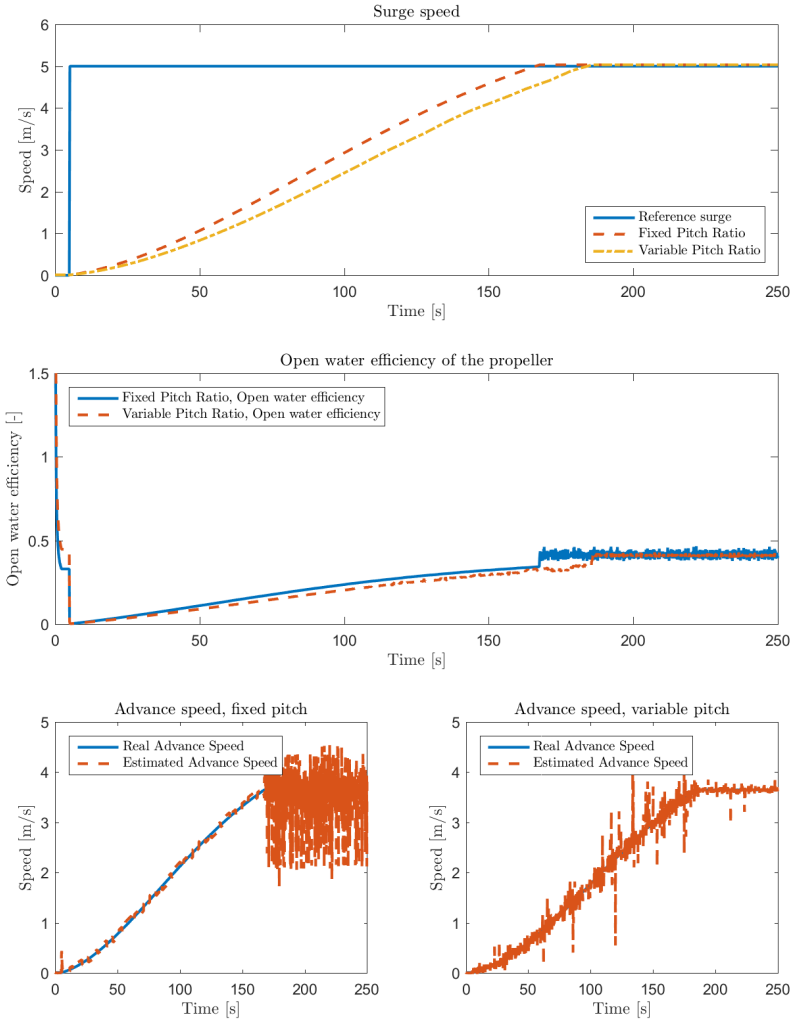

Figure 4.3: Results of test scenario three.

4.2.4 Test Scenario 4

The fourth test scenario mirrors much of the results in scenario two, with both scenarios having the fixed pitch propeller work better and more efficiently during the first acceleration. However, a large difference can be seen in the plot of the open water efficiency at around $t = [70, 110]$. The trends in the advance speed estimates in test scenario four are fairly similar with the trends in test scenario 3, but at the same time they do differ slightly. We can see that the fixed pitch mode controller works great with the advance speed estimation during acceleration, as they did in test scenario three. They also show the same fluctuations when the surge reference is met as they did when the reference speed in scenario three was reached. Something noteworthy is seen when the surge reference is decreasing. When the surge reference decreases, large values in the FPP's estimate can be seen. A zoomed in figure of the FPP's advance speed estimate with the same axis dimenions as the controllable pitch controller's estimate can be seen in the appendix (A.1).

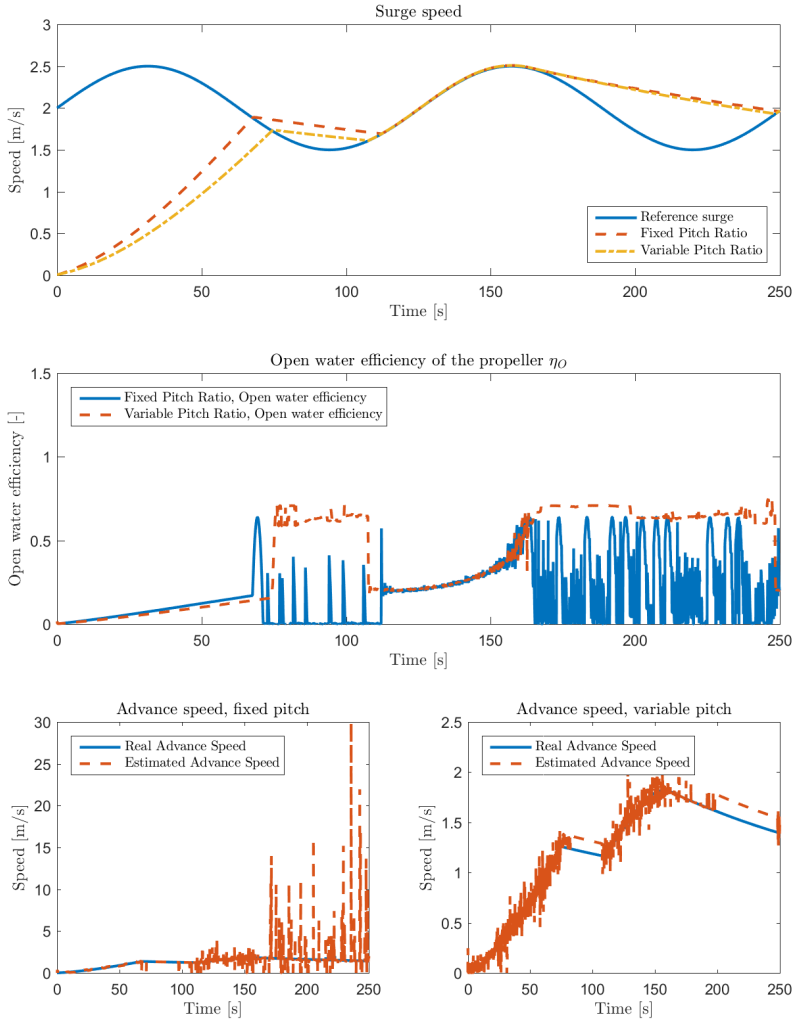

Figure 4.4: Results of test scenario four.

Chapter 5

Discussion

5.1 Test Scenario 1

Looking at the results in section 4.2.1 there are several issues that needs commenting. An example being the peak in open water efficiency at around $t = 0$. In figure 5.1 the open water efficiency of both propeller modes has been plotted with $t = [0, 4]$. Keep in mind that the open water efficiency of the propeller is described as:

$$\eta_O = \frac{J}{2\pi}\frac{K_t}{K_q} \tag{5.1}$$

In figure 5.1 it can be seen that the torque and thrust coefficients are relatively the same close to the start as they are as time increases, this suggests that they are not the reason for the spike in open water efficiency. The plot of the advance ratio however, has a large value close to $t = 0$ and quickly drops in the same time frame as the open water efficiency drops. One can therefore argue that the advance ratio is the reason for this peak. The advance ratio is described in (2.4), and by looking at figure 5.2 it is possible to see that the reason why the advance ratio peaks close to $t = 0$ is because of the low values of n. As the propeller starts to turn, the open water efficiency values quickly enters normal operating range. Another issue which can be seen in figure 5.2, is the sudden jump in the propeller's shaft speed. This applies to both the fixed pitch propeller and the controllable pitch propeller. The reason for this can be attributed to the discrete nature of the simulation. By looking at the enhanced torque plot in figure 5.3 it is clear that in the first time step, with the engine producing torque, the propeller is still at zero RPS. Which is why the propeller torque is also zero. Since the change in RPS is given by equation (2.7), a huge jump in RPS is observed when Q_p is low and the Q_m is comparatively very high. Once $Q_m \approx Q_p$ the RPS stops increasing as rapidly, as should be expected looking at equation (2.7). This phenomenon is also another reason for why the fixed pitch propeller reaches the reference faster than the CPP. As seen in figure 5.5, during the first time steps of the ODE solver, the fixed pitch propeller has a higher desired RPS than the controllable pitch propeller, leading to a larger initial

output of motor torque, giving the fixed pitch propeller a head start on controllable pitch propeller. It is hard to tell how much this head start has affected the FPP's performance. Another issue is that the fixed pitch propeller achieves the reference surge faster than the CPP and with greater efficiency. The faster surge acceleration is most likely because of the heightened efficiency. The reason this happens is because whilst the controllable pitch mode is optimized in a way to ensure greater efficiency, it does so by maximizing the efficiency subject to the desired thrust value. This might not necessarily lead to favourable input of P/D given the current shaft speed. As seen in figure 5.2 the pitch dynamics are magnitudes quicker than the propeller RPS dynamics, by choosing to set the pitch as high as the controller does early in the speed up process, there is placed additional torque on the propeller, compared to the fixed pitch of 0.8, leading to a slow down of the propeller shaft speed dynamics.

As shown in figure 5.4, it can be seen that even though the motor outputs has higher levels of torque with the controllable pitch mode propeller compared to the FPP that does not necessarily mean that the CPP is increasing its shaft speed more quickly. By looking at figure 5.4 it can be seen that the torque balance is more often in favour of the motor with the FPP than with the glscpp. As seen in the third plot in figure 5.4, the controllable pitch case is more often found below the zero threshold and with larger negative values.

Another reason why the controllable pitch mode performs worse might be the more rapidly changing references, seen in figure 5.2. A more stable reference leads to less jumps in the torque balance making the torque values more stable as well. In figure 5.4 it can be seen that the fixed pitch torque values are a lot more stable than that of the CPP's torque values. A possible fix, and much needed improvement of this is better tuning of the controllers involved. Namely the speed controller and consolidated controller. This is further discussed in chapter 6.

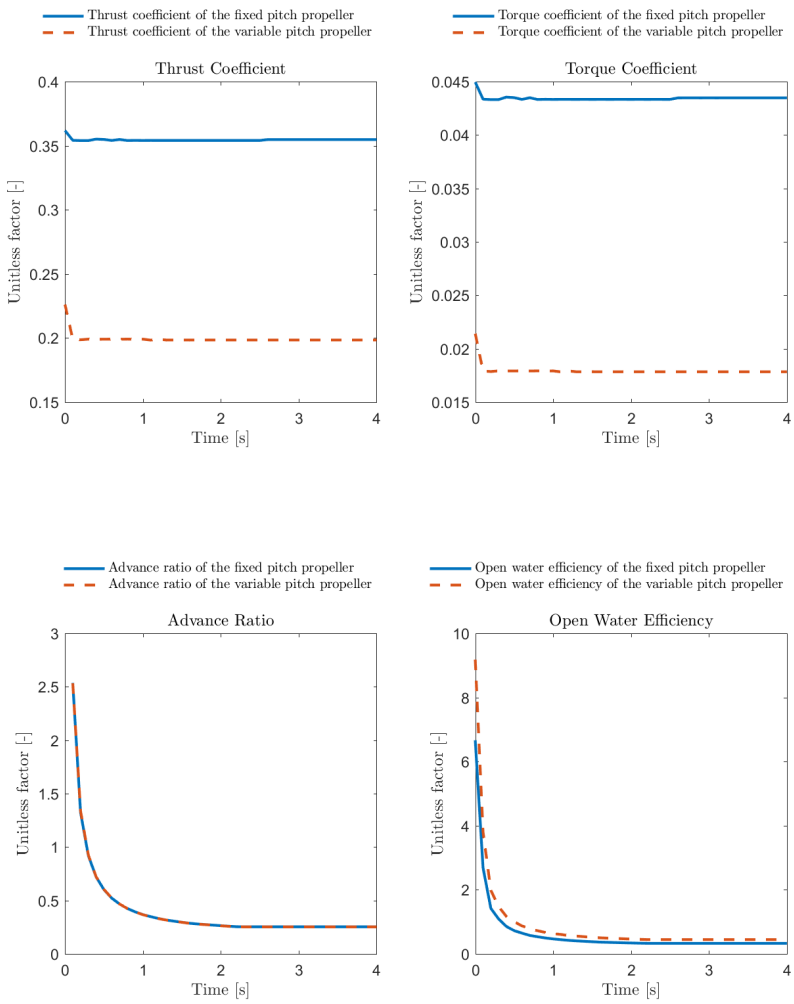

Figure 5.1: A zoomed in view of the open water efficiency in test scenario one and its components.

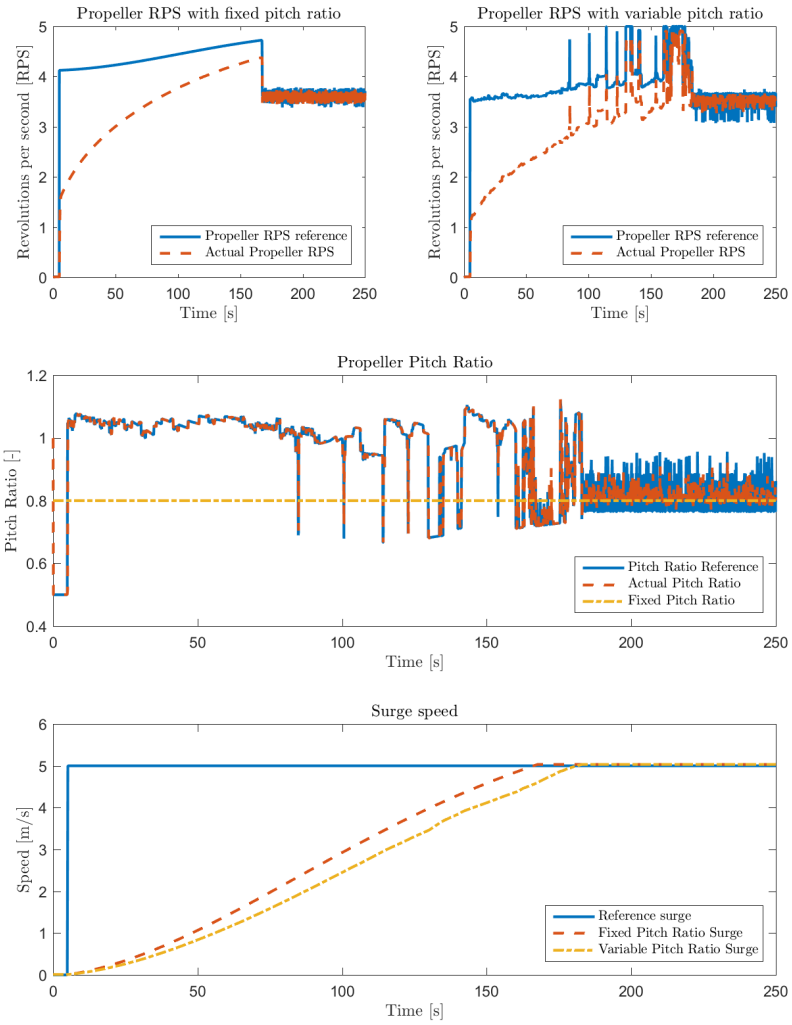

Figure 5.2: Plots showing the propeller outputs and the resulting surge speed.

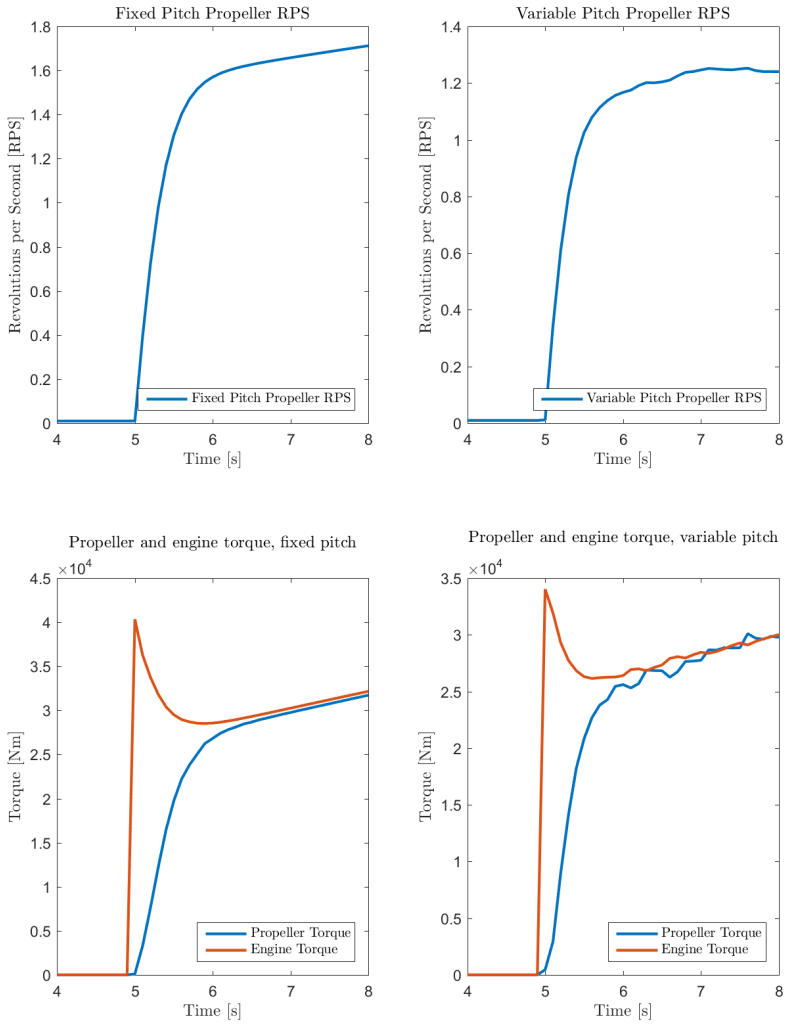

Figure 5.3: A plot of the engines' and the propellers' torque outputs

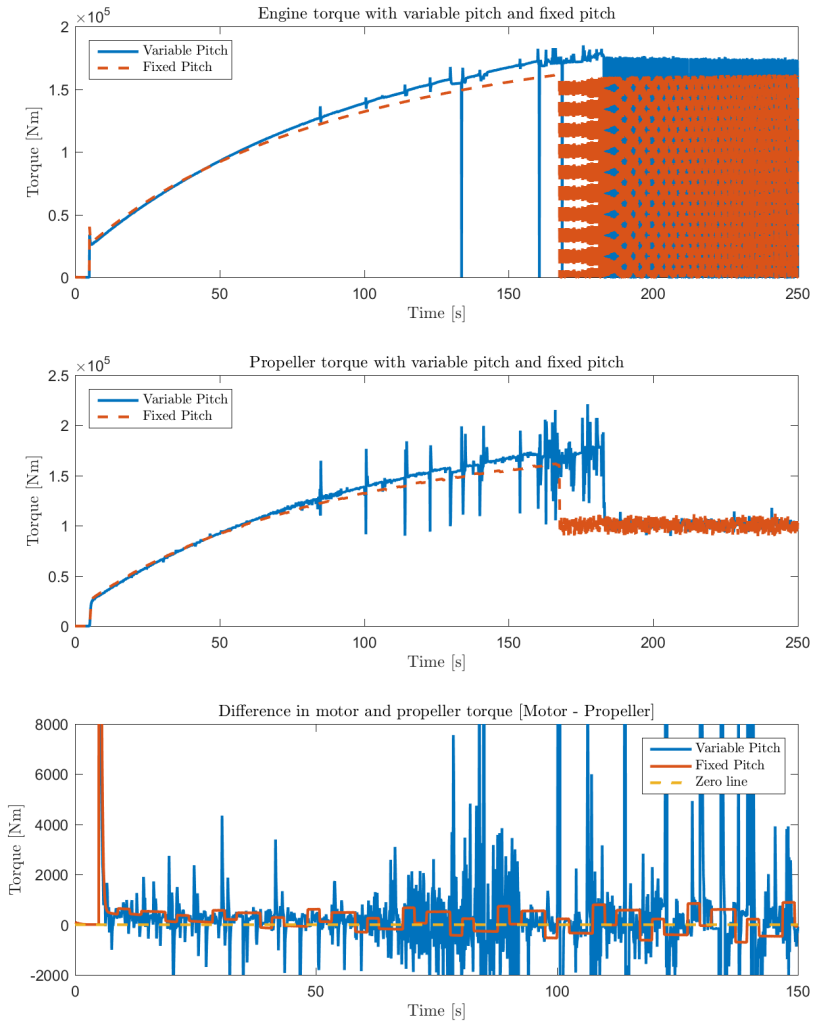

Figure 5.4: A plot of the engines' and the propellers' torque outputs, zoomed out and in comparison.

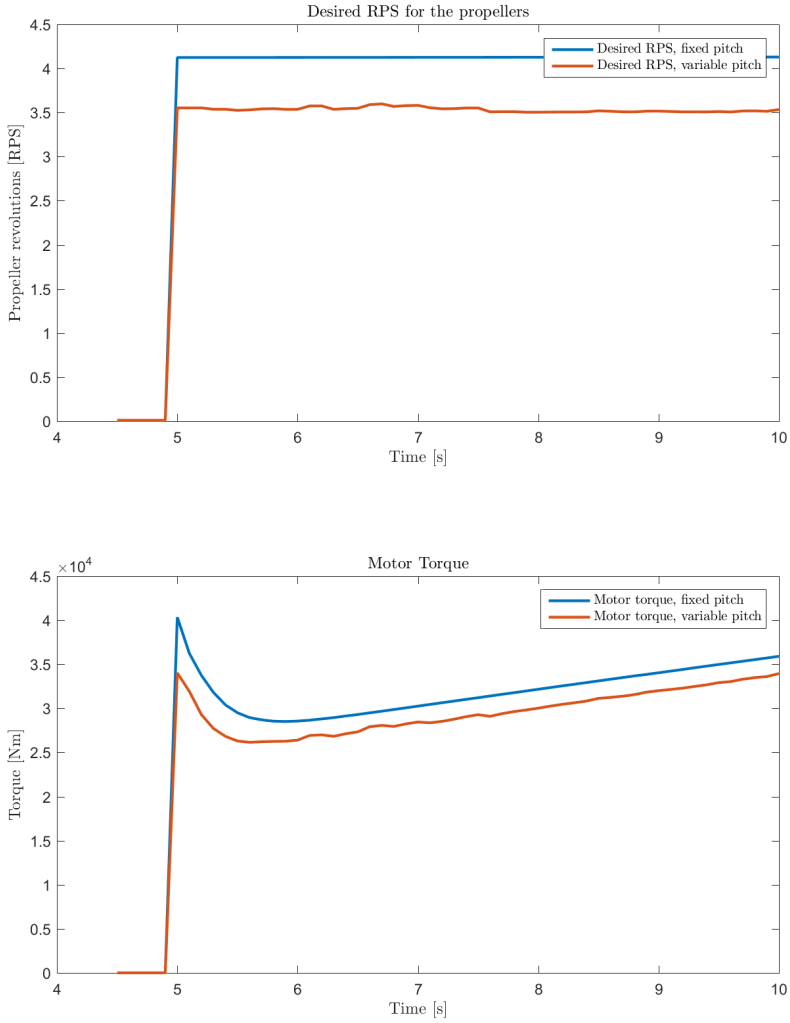

Figure 5.5: Desired RPS and produced Motor Torque during initial start phase.

5.2 Test Scenario 2

Looking at figure 4.2, we can clearly see the same trends presented in figure 4.1 and further discussed in chapter 5.1. The fixed pitch propeller achieves the reference surge quicker than the controllable pitch propeller. As seen in figure 5.6 we see that the controllable pitch ratio propeller is slower at increasing its RPS. This is because a bigger pitch diameter ratio leads to higher values of the propeller torque coefficient, which in turn leads to more resistance which must be overcome in order to turn the propeller. The controllable pitch propeller in test scenario two also suffers from the same disadvantage as the controllable pitch propeller in test scenario one (section: 5.1) does. It is clear when looking at figure 5.7 that the fixed pitch propeller has a much larger torque placed on it in the crucial first step of the simulation whilst the propeller torque load is still zero. However, with the reference surge being a sine curve the controllable pitch propeller is able to meet the rising reference at around 105 seconds, compared to the fixed pitch propeller which arrives at around 113 seconds. A major reason for this is that the controllable pitch propeller achieved the reference surge when the reference surge was at a lower point, meaning that the ship with the controllable pitch propeller had less kinetic energy to lose in order to meet the new, lower reference surge. The second time the surge reference is lower than the actual surge is however much more interesting as they both start of at the same speed, but the controllable pitch propeller is able to slow down its shaft speed quicker than the fixed pitch propeller. Looking to figure 5.6 and figure 5.8 it can be seen that by increasing its pitch, the propeller load is also increased leading to a more rapid decrease of propeller RPS and produced thrust. Which in turn leads to the controllable pitch propeller's ship being able to decelerate slightly faster than the fixed pitch propeller's ship. For the open water efficiency η_O it can be seen that the values for the fixed pitch propeller are more stable than the controllable pitch propeller's. These quick variations and peaks in the CPP's OWE curves are to be expected, as the rapid pitch dynamics can change the thrust and torque coefficients very quickly, evident in figure 5.9 and 5.10.

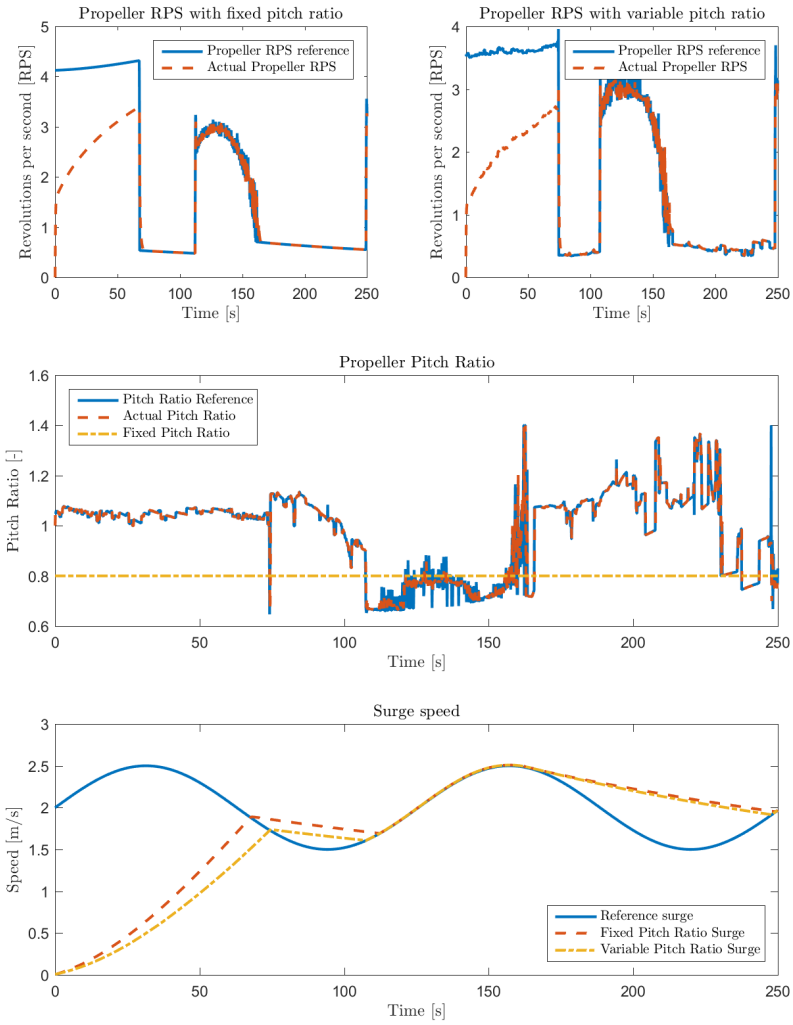

Figure 5.6: Outputs of the two propellers in test scenario 2

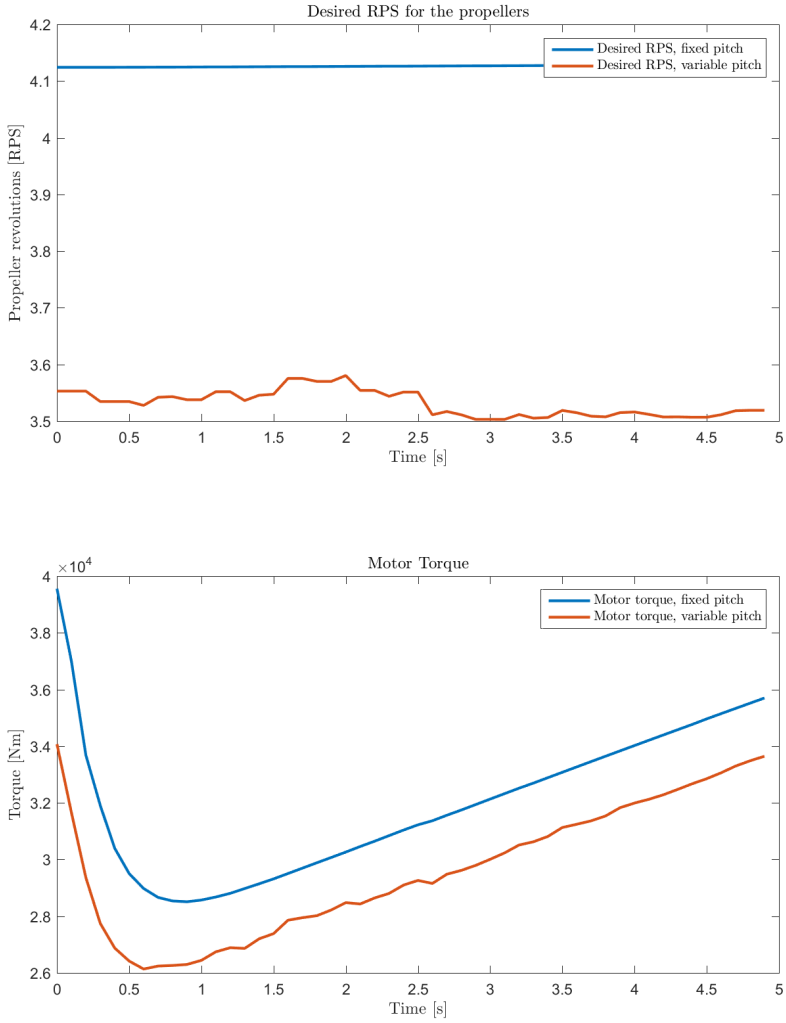

Figure 5.7: Desired RPS and produced Motor Torque during initial start phase.

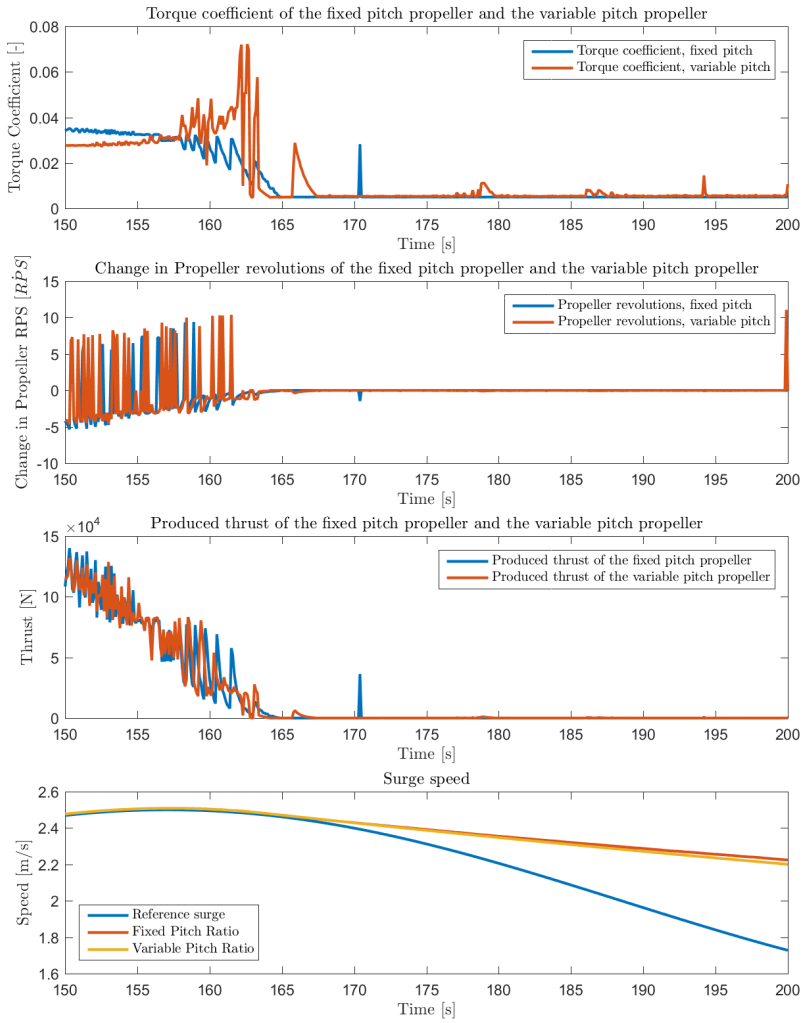

Figure 5.8: A plot of the propeller torque and its effect on the ship during the second breaking phase of test scenario 2.

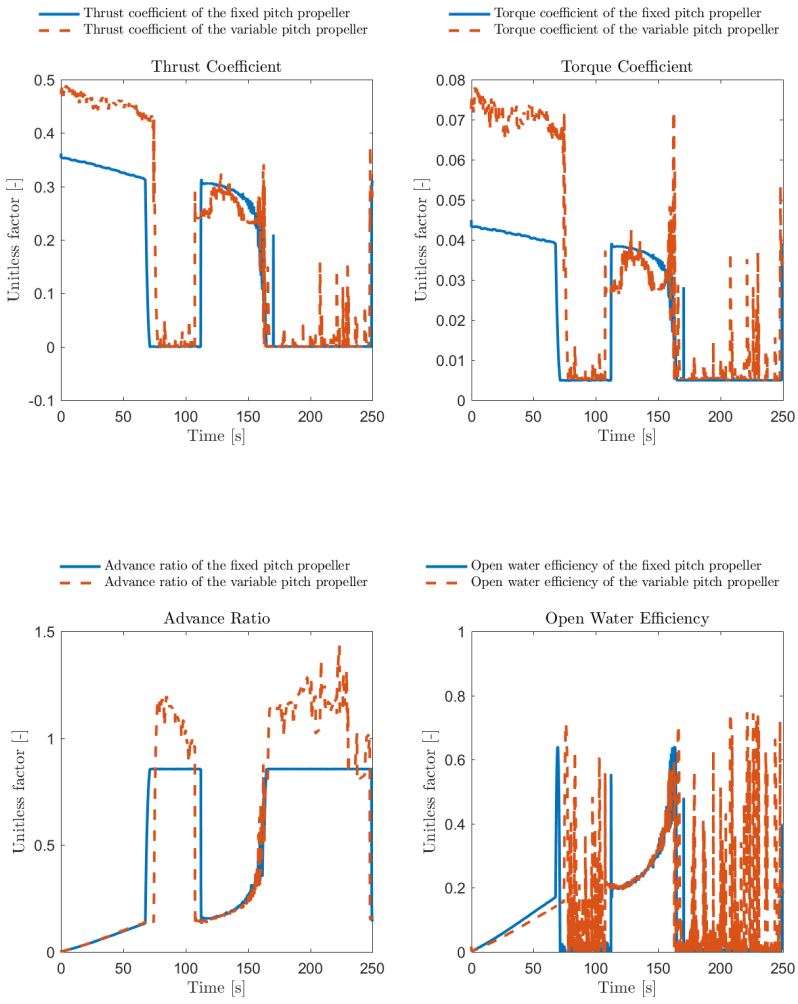

Figure 5.9: A plot showing the the respective thrust and torque coefficients of the two propellers, their advance ratios and also the resulting open water efficiency η_O.

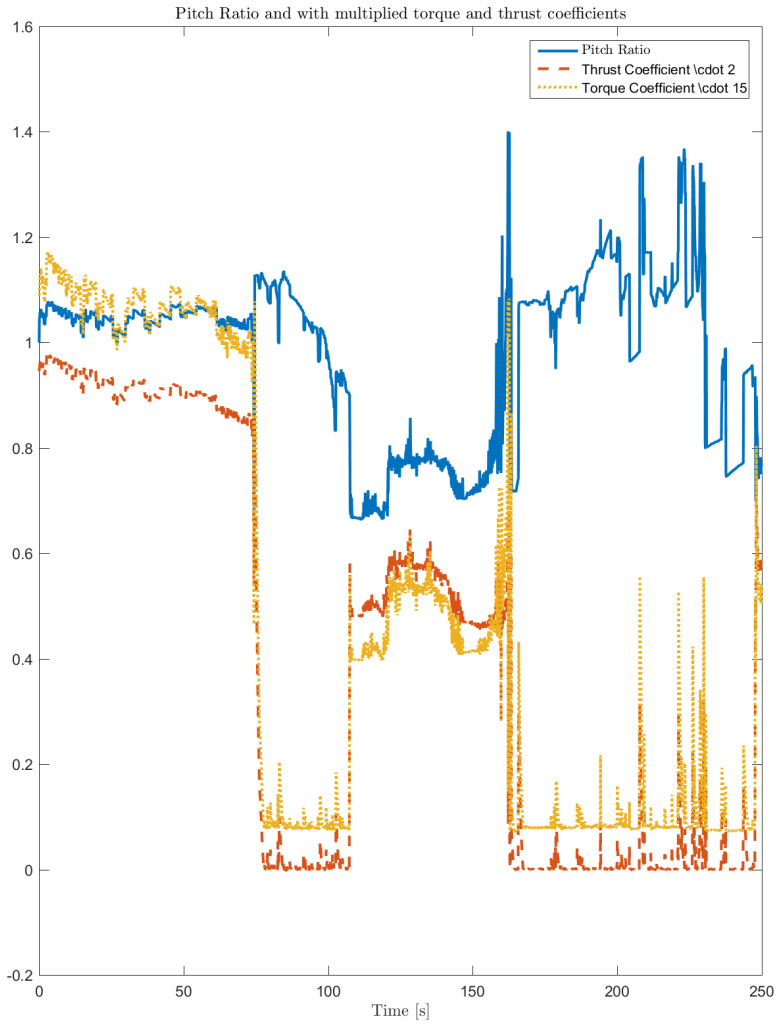

Figure 5.10: Pitch Diameter Ratio plotted with the Thrust and Torque Coefficients multiplied by 2 and 15 respectively.

5.3 Test Scenario 3

Looking at figure 4.3, one can see similar trends as in figure 4.1 for both the plot of the ships' surge speed and the plot of the propellers' OWE. As these trends have been discussed in both section 5.1 and section 5.2 they will not be discussed further here. There are however some interesting elements showing themselves in figure 4.3. Looking at the OWE plot of the CPP in figure 4.3 and comparing it with the OWE plot of the CPP in figure 4.1 one can observe that the plot in figure 4.3 is smoother. A reason for this might be that the fluctuating measurement of advance speed makes the consolidated controller give out more of a sporadic desired shaft speed, as can be observed in figure 5.11. It can be argued that the more fluctuating shaft speed reference acts as a filter, making the actual shaft speed more stable as observed in figure 5.11. The same fluctuations in the desired shaft speed for the FPP can also be observed in figure 5.12, however they are not as apparent before the surge reference is met. It also holds true for the CPP that the fluctuations in n are larger when the reference speed is met, although they do not increase as much as they do for the FPP. In figure 5.13 one can see that these fluctuations in desired shaft speed, ultimately creates fluctuations in the OWE of the propeller. The reason why these fluctuations in the desired shaft speed appears, might be due to the wavering nature of the advance speed estimate, $\hat{V}_a$, which can be observed in figure 4.3. This fits since the fluctuations in the advance speed estimates are also worse with the FPP. But why are the advance speed estimates so different from each other, and why are the FPP's estimates better than the CPP's during the start and worse at the end? Looking at figure 5.14 one can observe that the FPP's torque coefficient value is fairly stable up until about 160 seconds. The same can be said for the FPP's shaft speed seen in figure 5.12. This explains a stable estimate, as $\hat{V}_a$ is estimated from the torque equation (3.6). As the reference surge is met, the FPP's torque coefficient and shaft speed starts to fluctuate. This might also be why the FPP's advance speed estimates fluctuate when the reference is reached. It could even explain why the FPP's $\hat{V}_a$ fluctuate more than the CPP's. Because the FPP has about 50% larger fluctuations in shaft speed when the holding the surge reference. For the CPP the advance speed estimate's fluctuation is somewhat similar the entire way, except for some peaks that can be explained by MATLAB solver errors.

It can also be noted that in the case of the CPP, as seen in figure 5.15 the controller using the estimate is a few seconds slower than the controller using the measured advance speed. This too might be explained by the filter effect on the shaft speed, created by using the estimate. As one can observe in figure 5.11 the CPP with estimated advance speed is a little bit slower at reaching the high RPS levels.

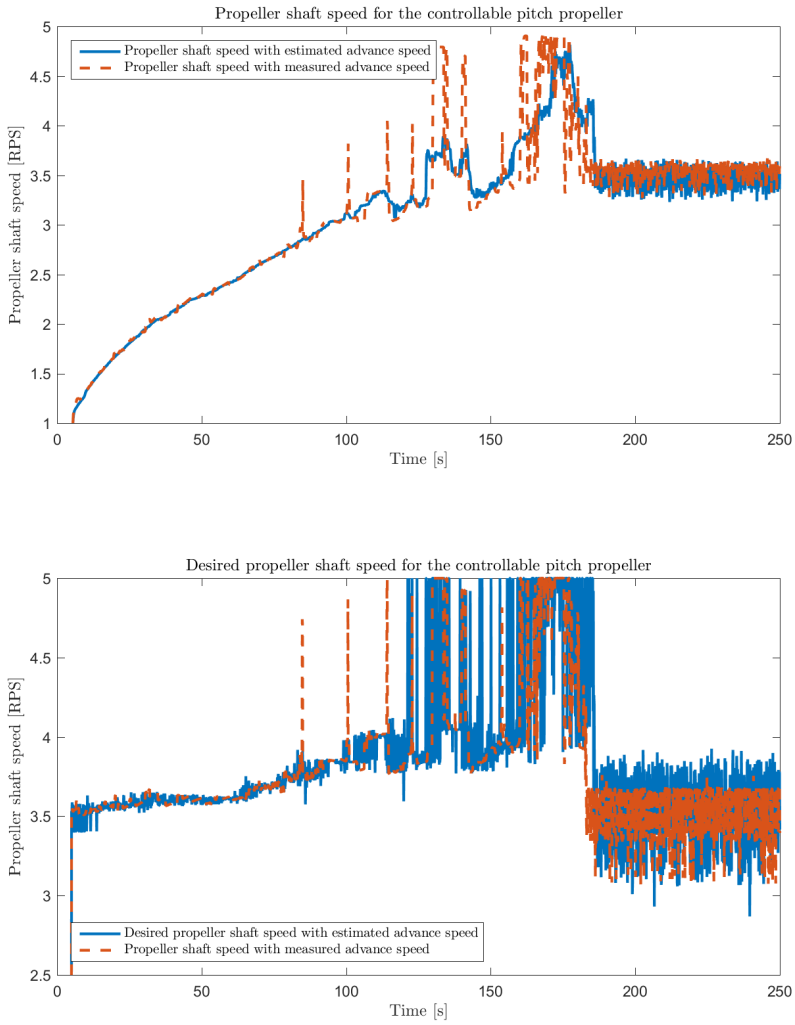

Figure 5.11: Plot of the shaft speed and desired shaft speed of the controllable pitch propeller with measured and estimated advance speed.

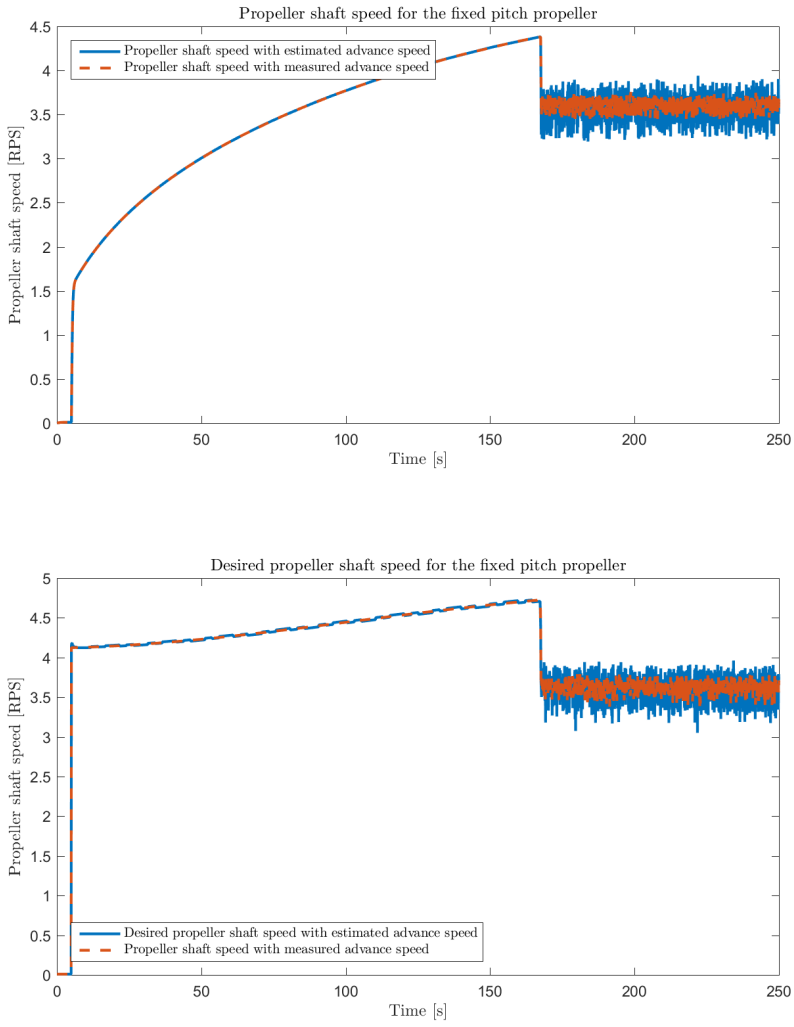

Figure 5.12: Plot of the shaft speed and desired shaft speed of the fixed pitch propeller with measured and estimated advance speed.

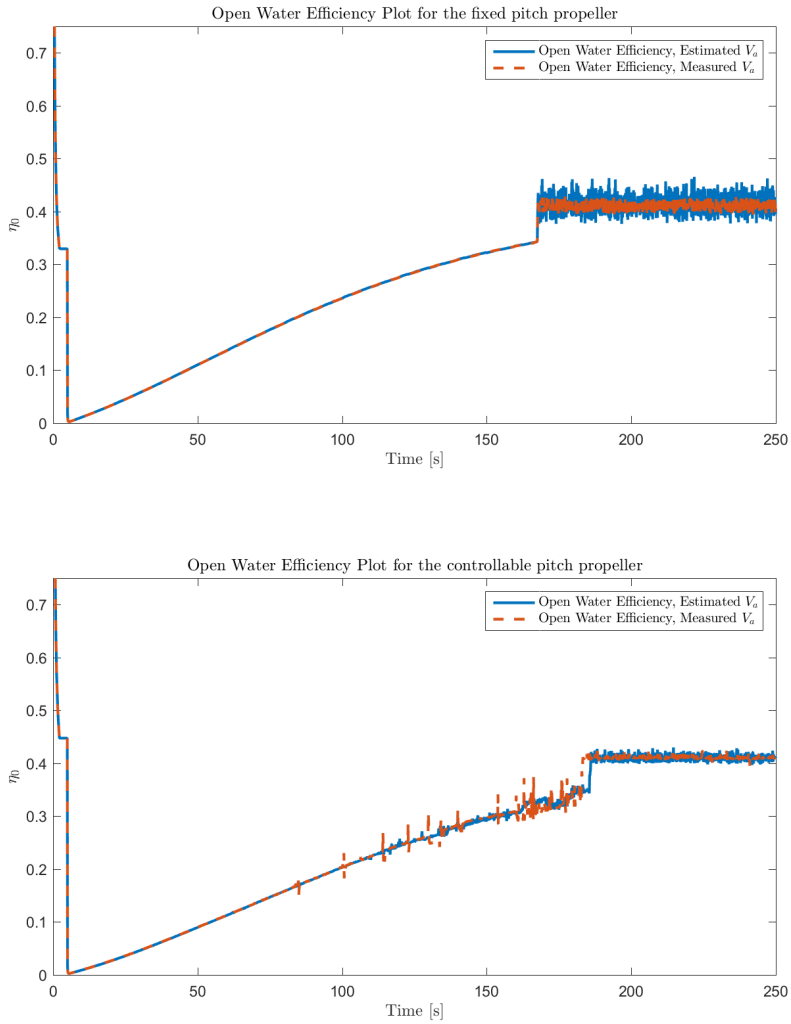

Figure 5.13: Plot of the open water efficiency of both the fixed and controllable pitch propeller, comparing OWE from simulations with both measured and real advance speed V_a.

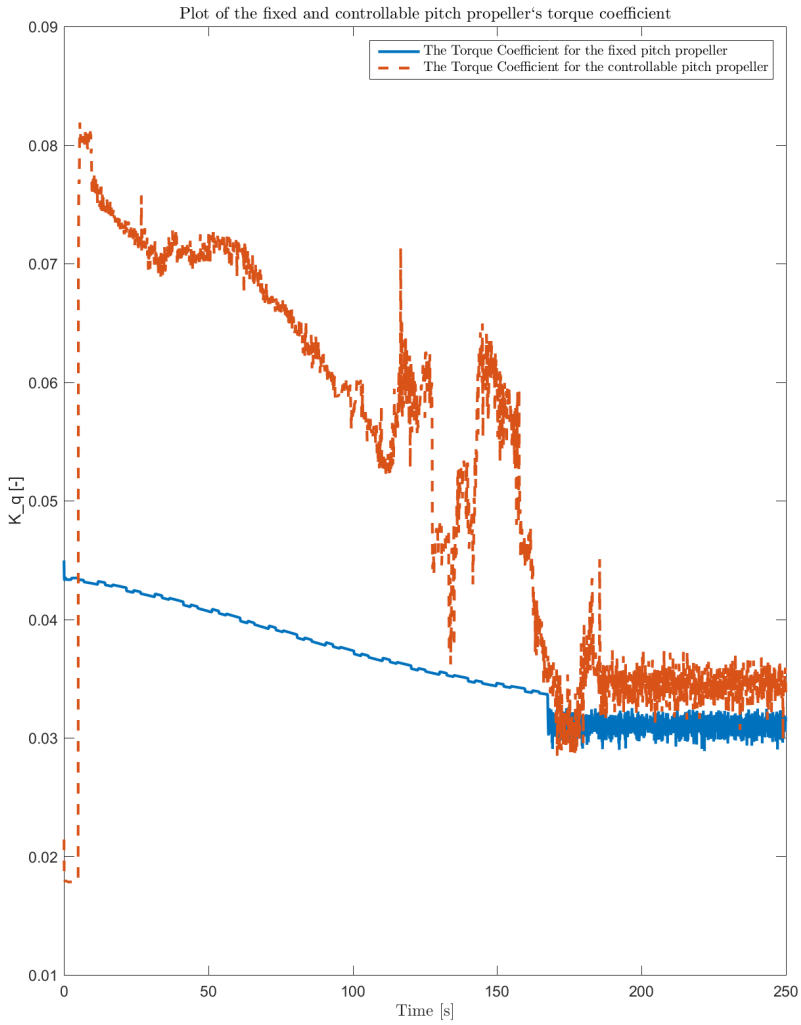

Figure 5.14: A plot of the torque coefficient for both the FPP and CPP.

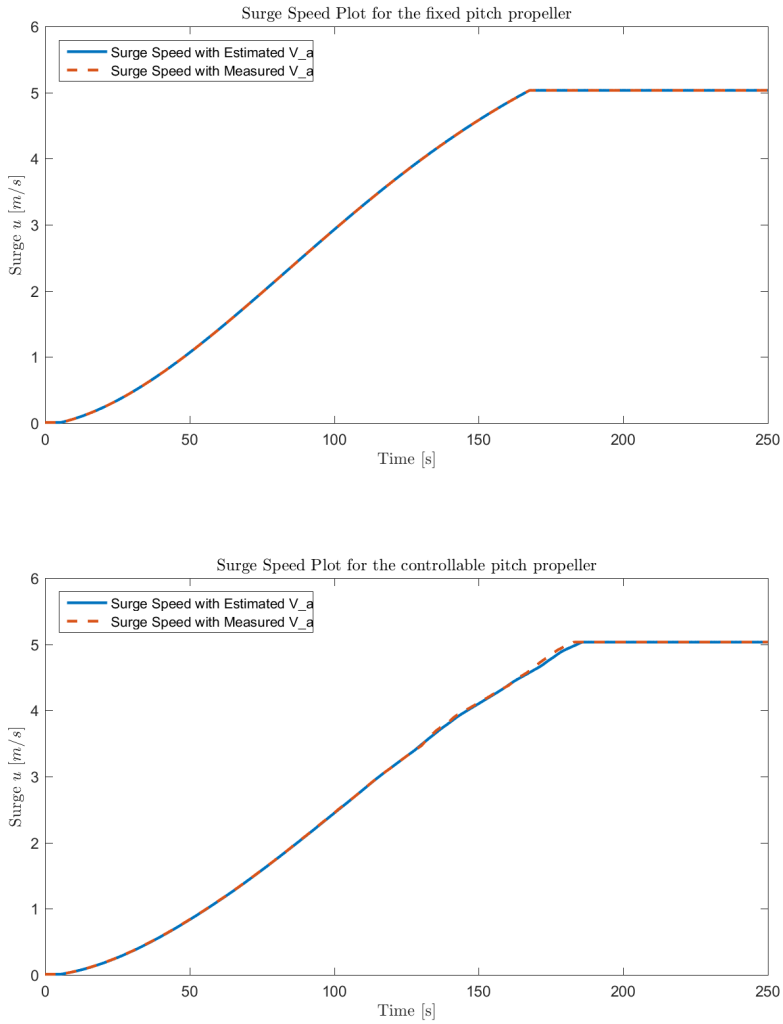

Figure 5.15: Plot of the resulting surge speed of both the fixed and controllable pitch propeller, comparing surge velocity from simulations with both measured and real advance speed V_a.

5.4 Test Scenario 4

The surge plot in figure 4.4 shows the same trends as the surge plot in figure 4.2. By that the fixed pitch propeller is faster before the reference is met, but is slower to respond to a decrease in reference surge. However, the surge plots differ slightly from each other. This is easier to notice when looking at the comparative surge plot in figure 5.16. Here one is able to see, that the controller is better able to decrease the ships' surge velocity using a measured value of V_a than it is with the estimate $\hat{V}_a$. A reason for this can be seen in figure 5.17. As it is apparent, especially in the case of the FPP is that the peaks in $\hat{V}_a$ causes peaks in the desired shaft speed n_d. Which in return causes the shaft speed to stay at higher levels of RPS for longer than is the case with the measured, $\bar{V}_a$. The same phenomenon can be said to hold true for the CPP case, although the effects are not as severe as with the FPP. A possible cause for why the FPP fares worse in this regard is that some of its $\hat{V}_a$ values shows traces of MATLAB solver errors. It is likely that these errors have had a negative effect on the FPP's results. Looking at figure 5.18 one can see the resulting advance speed estimate in the CPP scenario. The estimate is a bit rough, but works well enough for the control purposes in this thesis as can be seen in figure 5.16. However, the estimator had to rely a bit on its fail safe mechanism mentioned in section 3.4. Evident by the estimate being exactly a $\frac{4}{5}$ fraction of the ships' surge speed at certain intervals, most notably between about 200 and 250 seconds.

One can also observe that the use of an advance speed estimate has an effect on the OWE of the two propellers. Most notably perhaps the CPP, which has a greater OWE during slowing down of the surge. It is during this period that the FPP's OWE is showing a difference for the measured and estimated advance speed. The reason why the FPP differs, might the same reason why it also uses a longer time slowing down in surge. The $\hat{V}_a$ being bigger than the actual V_a and having peaks which also affects the shaft speed, has ripples reaching the OWE. Since the FPP's OWE is only a function of the shaft speed and advance speed this makes sense.

A reason why the CPP has a higher OWE during the slow downs might be that as one is able to see in figure 5.19, the measured value of $\bar{V}_a$ the K_t coefficients value is often zero or close to it when $t \approx [75,\ 110]$ and $t \approx [160,\ 250]$. Since we have that OWE is defined as (2.5), this can explain why the OWE values are often zero with the measured $\bar{V}_a$ and not with the estimated $\hat{V}_a$.

It seems as using the estimate seems to have no negative effect on the ships' ability to follow its surge elsewhere in the simulation.

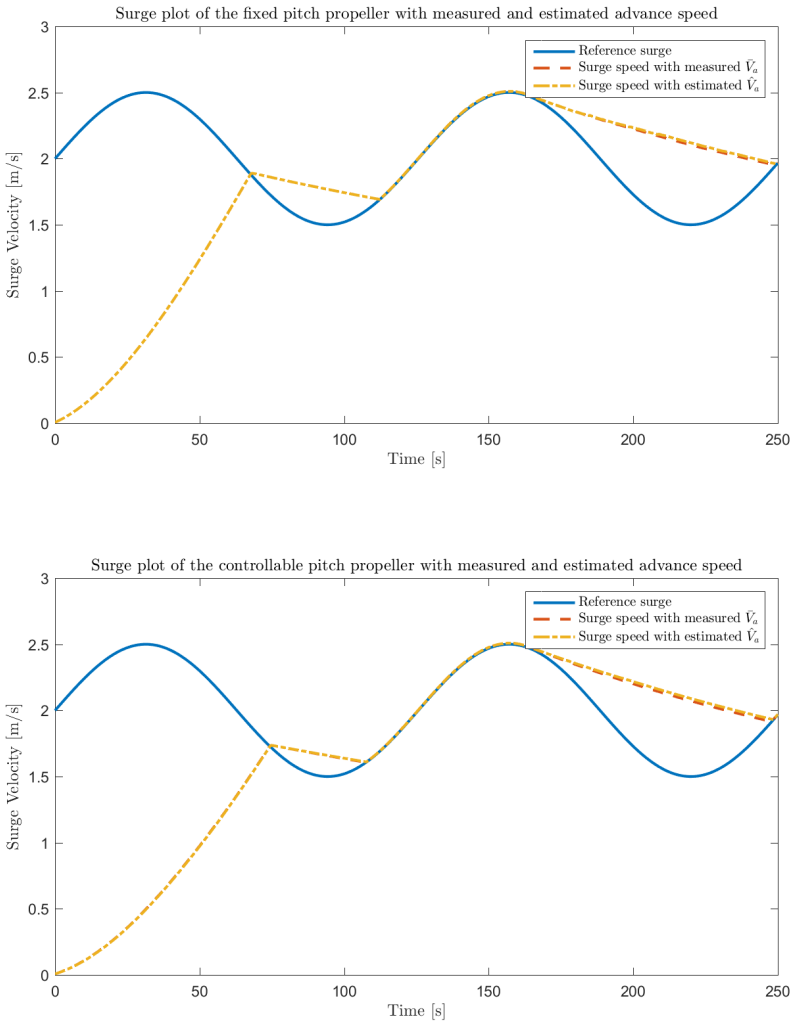

Figure 5.16: A plot showing the difference in surge speeds for both the CPP and FPP with measured and estimated advance speed, V_a.

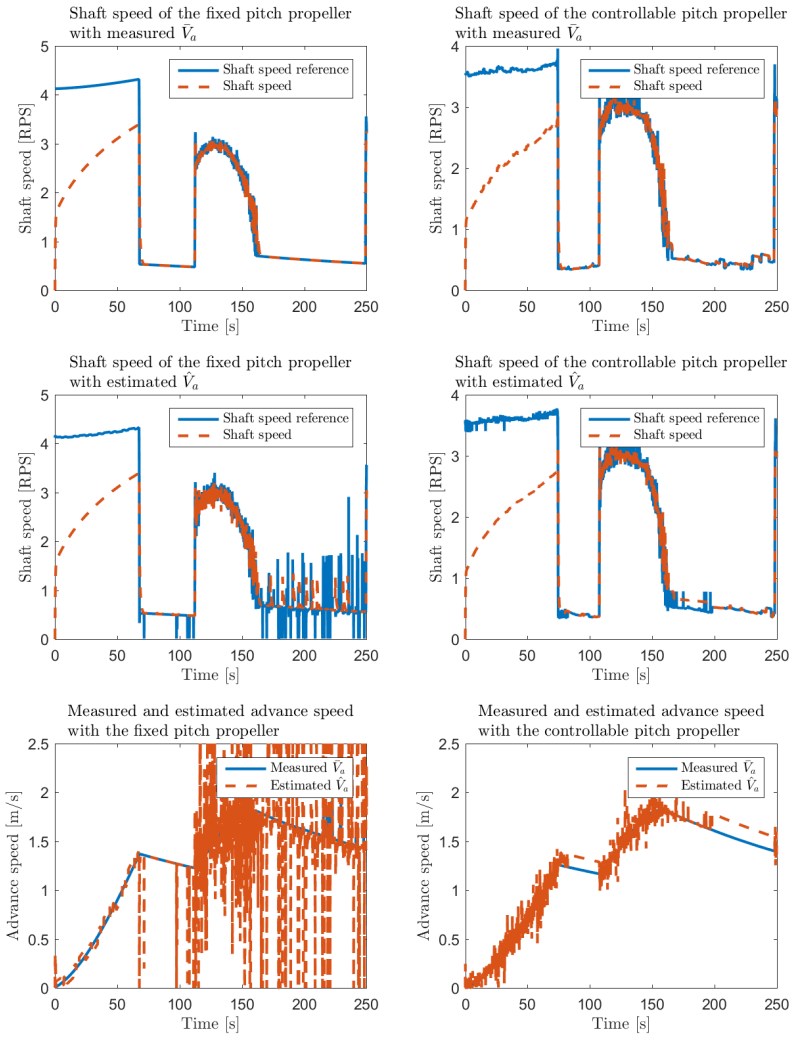

Figure 5.17: A plot showing the difference in propeller shaft speeds for both the CPP and FPP with measured and estimated advance speed, V_a.

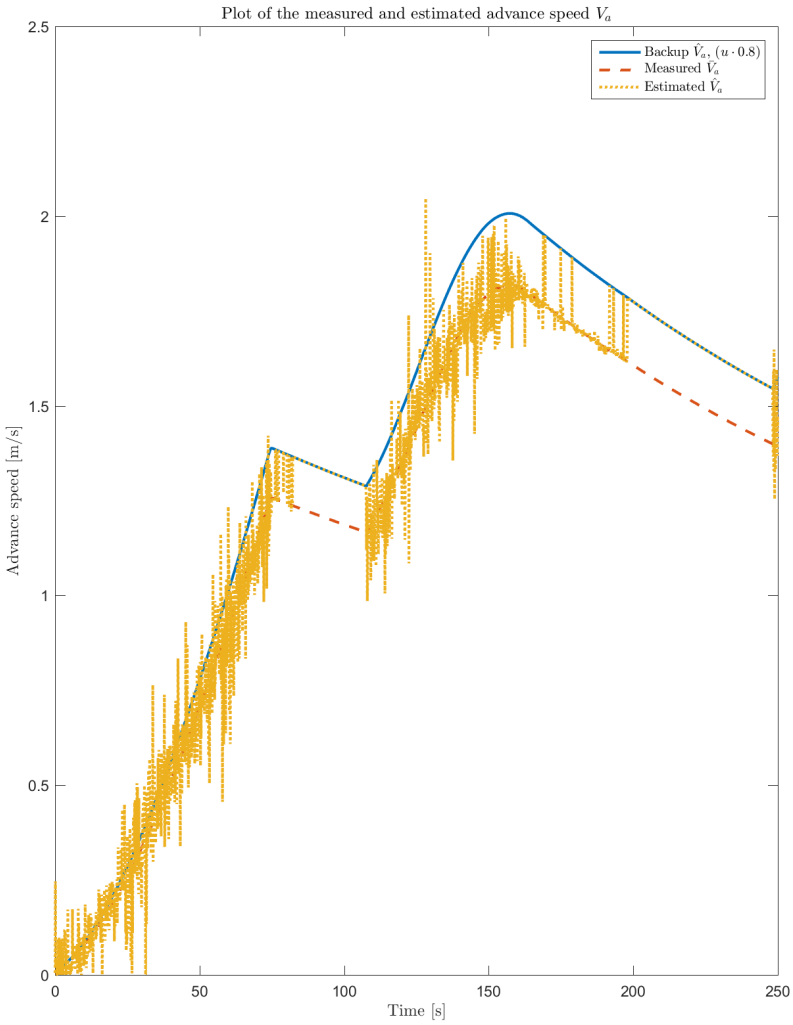

Figure 5.18: A plot of the advance speed estimation results of the CPP case.

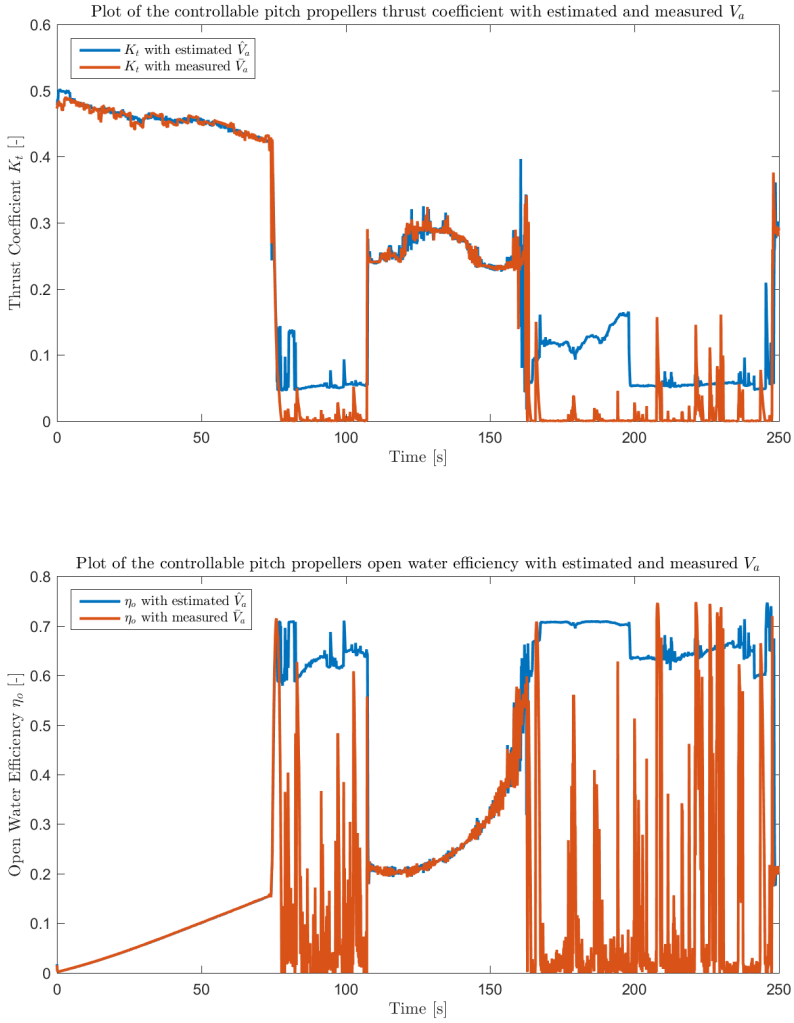

Figure 5.19: A plot showing the K_t coefficient of the CPP with both measured and estimated V_a.

5.5 Advance Speed Estimator

The advance speed estimator worked well enough to be used in the simulations in this thesis. Its effects were slightly negative with regards to acceleration in surge, but it did have some positive effects on the OWE, most notable in test scenario four (section 5.4).

In figure 5.20 and figure 5.21 the propellers except for the FPP in test scenario three, show no more trouble meeting their desired thrust rating with the estimated advance speed $\hat{V}_a$ than they do with the measured advance speed $\bar{V}_a$. The reason why the FPP struggles in test scenario three was discussed in section 5.3 and will therefore not be discussed here further.

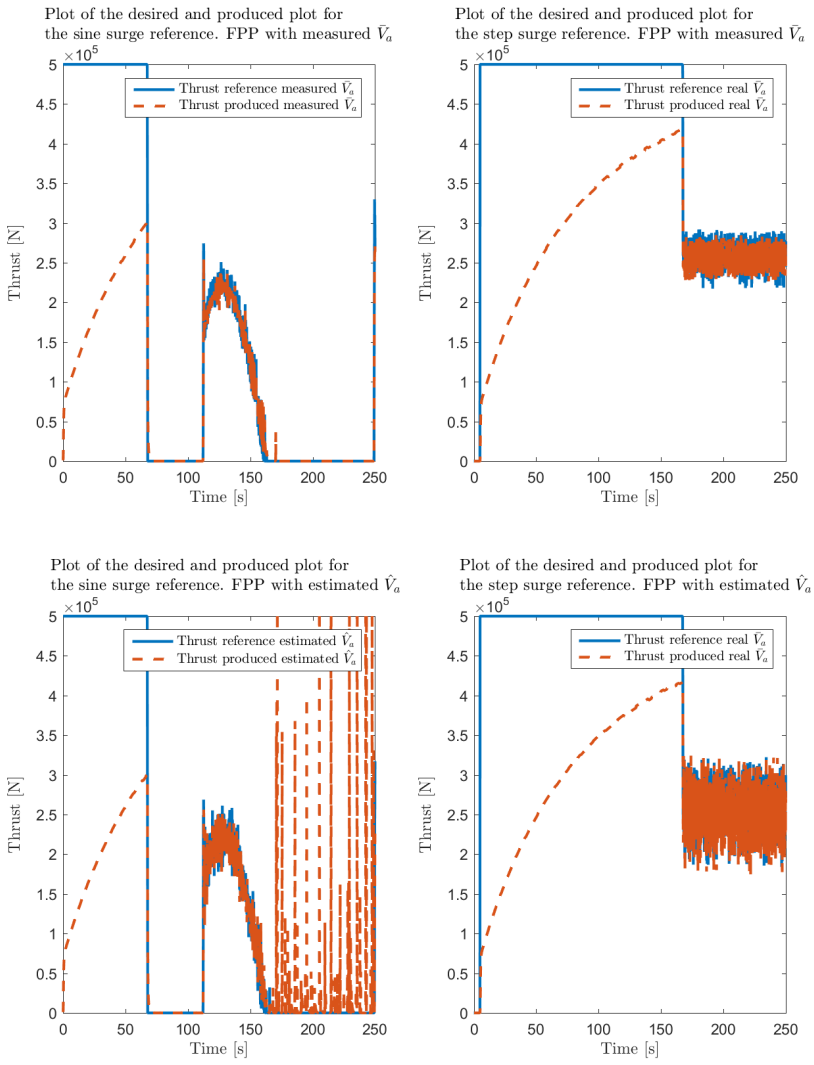

Figure 5.20: A plot showing the FPP's ability to match its desired thrust with estimated and measured advance speed

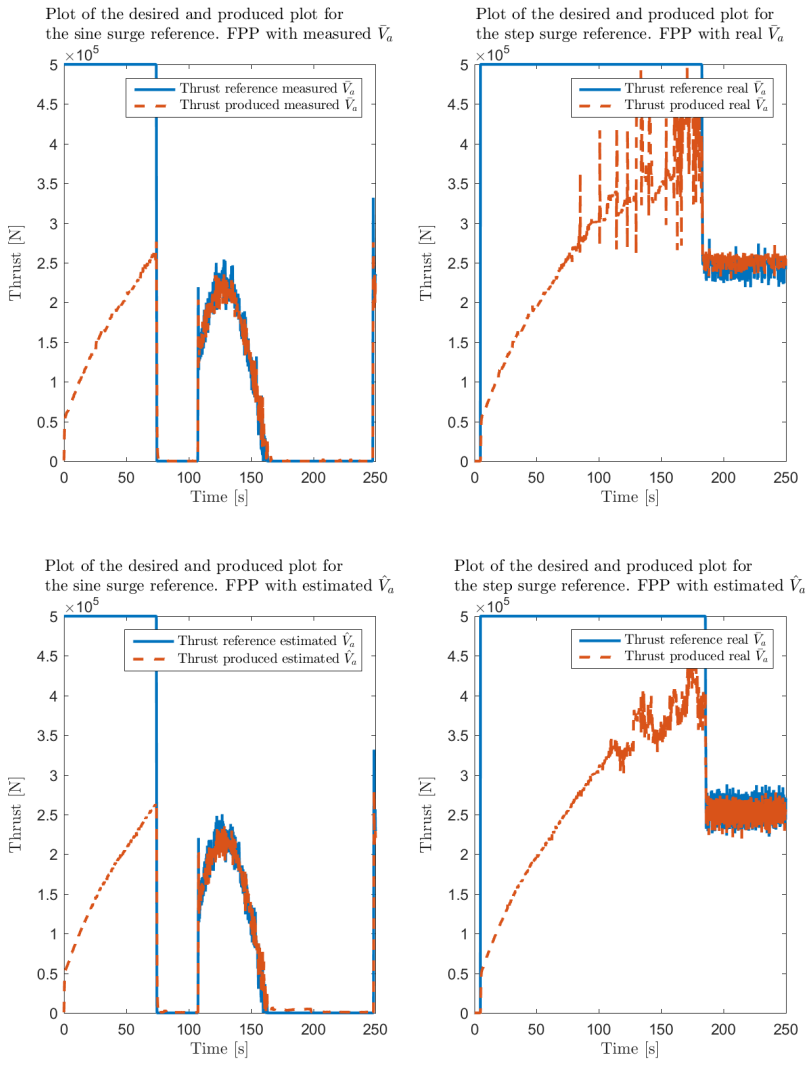

Figure 5.21: A plot showing the CPP's ability to match its desired thrust with estimated and measured advance speed

Chapter 6

Conclusion and Further Work

6.1 Conclusion

In conclusion, this thesis had two main objectives.

- Optimal control of shaft speed and pitch diameter ratio
- Advance speed estimation

With regards to the first objective, the thesis has not been successful in trying to create a controller capable of combining shaft speed n with pitch diameter ratio P/D in such a way as to optimally create the desired thrust. The primary cause of this is likely the large torque load of the propeller causing the shaft dynamics to be very slow. This makes optimizing for a single point very inefficient. The controller does manage however, to match its thrust reference (figure 5.21) reasonably enough to eventually match the reference surge (figures 4.1, 4.2, 4.3 and 4.4). At its best the consolidated controller managed to match the OWE of the controller operating with fixed pitch.
Pertaining to the advance speed estimation, this was accomplished. At least sufficiently for the controllers used in this thesi. As seen in figures 5.20 and 5.21, the thrust references for the propellers were met about as good with the estimated $\hat{V}_a$ as the measured $\bar{V}_a$. This is not saying the advance speed estimator could not use some tuning, its estimate can be somewhat choppy and might not be good enough for other controllers.

6.2 Further Work

As has been shown in this thesis, optimizing for a single point/thrust reference is not a viable strategy. A short term goal would be to make the optimizing be done for a path leading to the optimal point for the thrust reference. As creating an optimal path to the optimal point would ensure optimal performance throughout the thrust production, not only when $T_p = T_d$, this should be prioritized in future work. If implemented in simulations and presenting good results, scale testing should be considered as a long

term goal.
In the short term, investigation into improving the advance speed estimate should also be undertaken, if better tuned it is believed that this estimator could provide sufficient estimates for precise thrust production and ship control.
Besides the scale testing, other long terms goals should include trying to expand both the estimator and consolidated controller to work in all four propeller quadrants. This will have to be done if the methods should ever be implemented on full size ships. Expanding on this, the estimator and controller should also be made capable to work under conditions with in and out of water effects and cavitation.

Another long term goal, should be do to proper open water tests on a controllable pitch propeller or get the results from on in order to use more accurate values for the thrust and torque coefficients K_t and K_q.

Appendix A

Figures

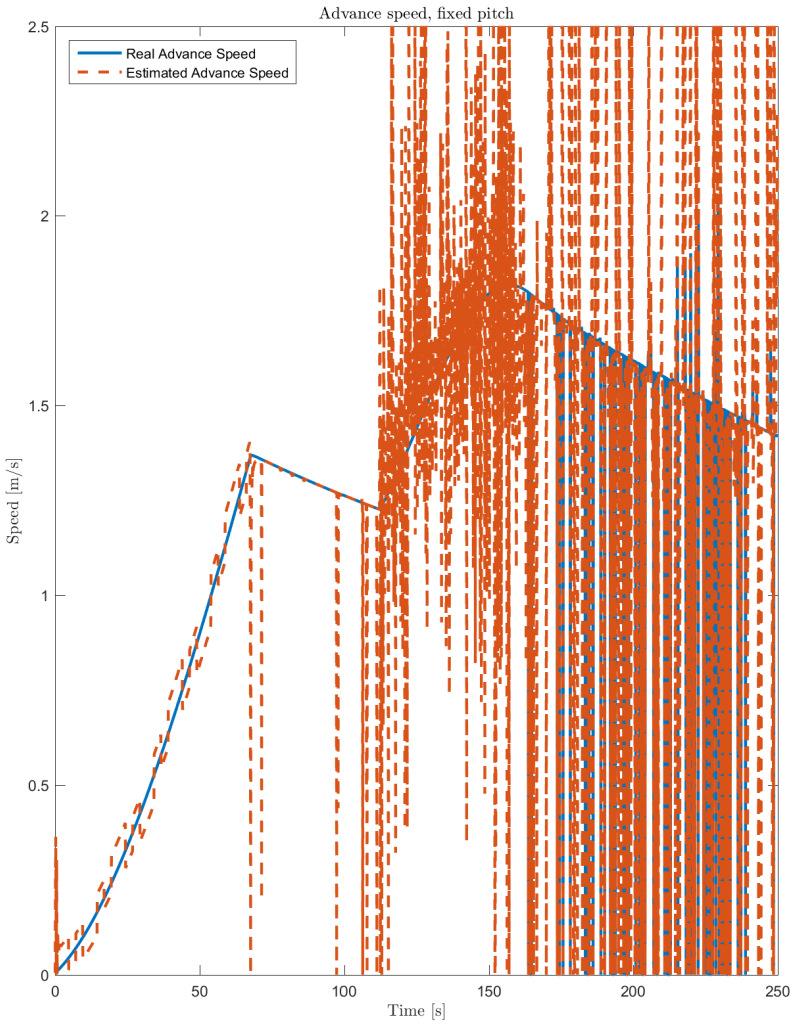

Figure A.1: Zoomed in view of the advance speed estimate with the fixed pitch mode controller

TABLE 1

Coefficients and terms of the K_T and K_Q polynomials for the Wageningen B-screw Series for $R_n = 2 \times 10^6$. Reproduced from [1]

$$K_T = \sum_{s,t,u,v} C^T_{s,t,u,v} \cdot (J)^s \cdot (P/D)^t \cdot (A_E/A_O)^u \cdot (z^v)$$

$$K_Q = \sum_{s,t,u,v} C^Q_{s,t,u,v} \cdot (J)^s \cdot (P/D)^t \cdot (A_E/A_O)^u \cdot (z^v)$$

K_T $C^T_{s,t,u,v}$	s (J)	t (P/D)	u (A_E/A_O)	v (Z)	K_Q $C^Q_{s,t,u,v}$	s (J)	t (P/D)	u (A_E/A_O)	v (Z)
+0.00880496	0	0	0	0	+0.00379368	0	0	0	0
-0.204554	1	0	0	0	+0.00886523	2	0	0	0
+0.166351	0	1	0	0	-0.032241	1	1	0	0
+0.158114	0	2	0	0	+0.00344778	0	2	0	0
-0.147581	2	0	1	0	-0.0408811	0	1	1	0
-0.481497	1	1	1	0	-0.108009	1	1	1	0
+0.415437	0	2	1	0	-0.0885381	2	1	1	0
+0.0144043	0	0	0	1	+0.188561	0	2	1	0
-0.0530054	2	0	0	1	-0.00370871	1	0	0	1
+0.0143481	0	1	0	1	+0.00513696	0	1	0	1
+0.0606826	1	1	0	1	+0.0209449	1	1	0	1
-0.0125894	0	0	1	1	+0.00474319	2	1	0	1
+0.0109689	1	0	1	1	-0.00723408	2	0	1	1
-0.133698	0	3	0	0	+0.00438388	1	1	1	1
+0.00638407	0	6	0	0	-0.0269403	0	2	1	1
-0.00132718	2	6	0	0	+0.0558082	3	0	1	0
+0.168496	3	0	1	0	+0.0161886	0	3	1	0
-0.0507214	0	0	2	0	+0.00318086	1	3	1	0
+0.0854559	2	0	2	0	+0.015896	0	0	2	0
-0.0504475	3	0	2	0	+0.0471729	1	0	2	0
+0.010465	1	6	2	0	+0.0196283	3	0	2	0
-0.00648272	2	6	2	0	-0.0502782	0	1	2	0
-0.00841728	0	3	0	1	-0.030055	3	1	2	0
+0.0168424	1	3	0	1	+0.0417122	2	2	2	0
-0.00102296	3	3	0	1	-0.0397722	0	3	2	0
-0.0317791	0	3	1	1	-0.00350024	0	6	2	0
+0.018604	1	0	2	1	-0.0106854	3	0	0	1
-0.00410798	0	2	2	1	+0.00110903	3	3	0	1
-0.000606848	0	0	0	2	-0.000313912	0	6	0	1
-0.0049819	1	0	0	2	+0.0035985	3	0	1	1
+0.0025983	2	0	0	2	-0.00142121	0	6	1	1
-0.000560528	3	0	0	2	-0.00383637	1	0	2	1
-0.00163652	1	2	0	2	+0.0126803	0	2	2	1
-0.000328787	1	6	0	2	-0.00318278	2	3	2	1
+0.000116502	2	6	0	2	+0.00334268	0	6	2	1
+0.000690904	0	0	1	2	-0.00183491	1	1	0	2
+0.00421749	0	3	1	2	+0.000112451	3	2	0	2
+0.0000565229	3	6	1	2	-0.0000297228	3	6	0	2
-0.00146564	0	3	2	2	+0.000269551	1	0	1	2
					+0.00083265	2	0	1	2
					+0.00155334	0	2	1	2
					+0.000302683	0	6	1	2
					-0.0001843	0	0	2	2
					-0.000425399	0	3	2	2
$R_n = 2 \times 10^6$					+0.0000869243	3	3	2	2
					-0.0004659	0	6	2	2
					+0.0000554194	1	6	2	2

Figure A.2: K_t and K_q table courtesy of M.M Bernitsas (1981)

Bibliography

, 2010. Mss. marine system simulator. Online; accessed 03.09.2015.
URL http://www.marinecontrol.org/

Fossen, T. I., 1994. Guidance and Control of Ocean Vehicles. Wiley.

Fossen, T. I., 2011. Handbook of marine craft hydrodynamics and motion control. Wiley.

Fossen, T. I., 2015. Lecture notes: Ttk 4190 guidance and control of vehicles. [Image from lecture slides of chapter 1].

Froudedude, 2009. Open water video. [Online; accessed January 12, 2016].
URL https://www.youtube.com/watch?v=vmhcKm6I1Mo

K. J. Rawson, E. C. T., 1976. Basic Ship Theory: Hydrostatics and strength, 2nd Edition. Prentice Hall Press.

Luca Pivano, Tor Arne Johansen, Ø. N. S., 2009. A four-quadrant thrust estimation scheme for marine propellers: Theory and experiments. IEEE Control Systems Technology 17.

MAN Marine Engines & Systems, 2012. Diesel-electric propulsion plants. [Online; accessed January 12, 2016].
URL http://marine.man.eu/docs/librariesprovider6/marine-broschures/diesel-electric-drives-guideline.pdf?sfvrsn=0/

M.M Bernitsas, D. Ray, P. K., 1981. k_t,k_q and efficieny curves for the wageningen b-series propellers. Naval Architecture & Marine Engineering (NA&ME) 237.

Schottel, 2010. Scp controllable-pitch propeller. [Online; accessed January 12, 2016].
URL http://www.schottel.de/marine-propulsion/scp-cp-propeller/

Sponberg, E., 2001. c_b illustration.

Taylor, D., 1943. The speed and Power of Ships, a Manual of Ship Propulsion. Wiley.